

 M 2016

**U. PORTO**  
FEUP FACULDADE DE ENGENHARIA  
UNIVERSIDADE DO PORTO

# **DEVELOPMENT AND CHARACTERIZATION OF POLY(LACTIC ACID)/FISH GELATINE ELECTROSPUN MEMBRANES FOR PERIPHERAL NERVE REGENERATION**

**MARIANA BRANCO MARINHEIRO FERREIRA DE SOUSA**  
DISSERTAÇÃO DE MESTRADO APRESENTADA  
À FACULDADE DE ENGENHARIA DA UNIVERSIDADE DO PORTO EM  
ENGENHARIA BIOMÉDICA

A Dissertação intitulada

“Development and Characterization of Poly(lactic acid)/Fish Gelatine  
Electrospun Membranes for Peripheral Nerve Regeneration”

foi aprovada em provas realizadas em 17-10-2016

o júri

  
Presidente Prof. Doutor Miguel Fernando Paiva Velhote Correia  
Professor Auxiliar do Departamento de Engenharia Eletrotécnica e de Computadores da FEUP  
- U.Porto

  
Prof.ª Doutora Ana Colette Pereira de Castro Osório Maurício  
Professora Associada c/Agregação da Instituto de Ciências Biomédicas Abel Salazar da U.  
Porto

  
Prof. Doutor José Domingos da Silva Santos  
Professor Associado do Departamento de Engenharia Metalúrgica e de Materiais da FEUP -  
U.Porto

O autor declara que a presente dissertação (ou relatório de projeto) é da sua exclusiva autoria e foi escrita sem qualquer apoio externo não explicitamente autorizado. Os resultados, ideias, parágrafos, ou outros extratos tomados de ou inspirados em trabalhos de outros autores, e demais referências bibliográficas usadas, são corretamente citados.

Mariana Branco Marinheiro Ferreira de Sousa  
Autor - Mariana Branco Marinheiro Ferreira de Sousa

Faculdade de Engenharia da Universidade do Porto



**Development and characterization of poly(lactic acid)/fish gelatine electrospun membranes for peripheral nerve regeneration**

Mariana Branco Marinheiro Ferreira de Sousa

Master in Biomedical Engineering

Supervisor: Prof. José Domingos Santos

Co-Supervisor: Prof. Vitor Sencadas

September, 2016

Mariana Branco Marinheiro Ferreira de Sousa, 2016

# Abstract

Injuries to the peripheral nervous system are a major cause for permanent disabilities with a strong effect on a diminished quality of life. The neurological sequels left by this kind of injuries result in a diminished daily live activity as well as loss of work capabilities. Peripheral nerve injuries are the principal cause of disorders with devastating impact on quality of life of patients and affects a large part of the population over the world. Therefore, this has a socioeconomic impact. For those reasons, the surgery to repair the damage to the peripheral nerve is urgently needed as well as a medical challenge.

In recent years, various surgical techniques have been carried out to aid the regeneration and repair of damage in peripheral nerves. However, the functional recovery is usually incomplete. Thus, a promising alternative is to use natural and synthetic neural scaffolds in which tubular nerve guidance conduits (NGC) is the basic structure. Guidance channels provide a microenvironment and mechanical support, directing the axonal growth from the proximal to the distal nerve stumps. In addition, they are designed and fabricated to increase the number, speed and length of the regenerating nerves.

A very important factor for the fabrication of NGC is the biomaterials selection. Synthetic and natural polymers, such as poly(lactic acid) (PLA) and fish gelatine (GE), have received great attention and have been widely used in tissue engineering because their properties can be tailored and are inexpensive.

In addition to the material selection, fabrication methods are also critical for designing neural scaffolds. Electrospinning allows the production of nanofibrous scaffolds that offer optimal surface properties for cell attachment, proliferation and differentiation because they can potentially mimic the structure of natural extracellular matrix (ECM).

In this context, this work aimed the production of biomaterials that promote the peripheral nerve regeneration. In this way, electrospun membranes of PLA blended with fish gelatine were developed at five different weight ratios. Additionally, the potential of these membranes for peripheral nerve regeneration was characterized in terms of their physicochemical properties. In order to characterize the biological properties of the membranes produced, *in vitro* cytotoxicity assays were performed. These assays revealed that the electrospun membranes are biocompatible and the PG11 membranes was proven to be a good substrate for fibroblast adhesion and proliferation compared to pure PLA and GE, since their morphology and structure was improved.

**Keywords:** Electrospinning, fish gelatine, poly(lactic acid), peripheral nerve regeneration, tissue engineering.



# Resumo

As lesões do sistema nervoso periférico são uma das principais causas de incapacidade permanente e têm um impacto negativo na qualidade de vida dos pacientes. As sequelas neurológicas deixadas por este tipo de lesões comprometem as atividades do dia-a-dia, bem como as capacidades de trabalho. Estas lesões são a principal causa de doenças com impacto devastador na qualidade de vida dos pacientes, afetando uma grande parte da população no mundo inteiro. Desta forma, têm um elevado impacto sócio-económico. Por estas razões, a correção cirúrgica de lesões nos nervos periféricos representa uma necessidade médica urgente, bem como um grande desafio clínico.

Nos últimos anos, têm sido realizadas várias técnicas cirúrgicas para reparar e regenerar os nervos periféricos. No entanto, a recuperação funcional, normalmente, é incompleta. Assim, uma alternativa promissora é a utilização de tubos-guia, sintéticos e/ou naturais. Estes tubos-guia proporcionam um microambiente, suporte mecânico e direcionam o crescimento axonal. Além disso, são implementados para aumentar o número, a velocidade e o comprimento da regeneração nervosa.

Um fator muito importante para a fabricação dos tubos-guia é a seleção dos biomateriais. Polímeros sintéticos e naturais, como o ácido poli-láctico (PLA) e gelatina de peixe (GE), têm sido amplamente utilizados na área de engenharia de tecidos devido à possibilidade de adaptação das suas propriedades e o seu custo.

Além da seleção dos biomateriais, a escolha do método de processamento também é um fator crítico na conceção de tubos-guia. A técnica de *electrospinning* permite a produção de *scaffolds* nanofibrosos que apresentam ótimas propriedades superficiais para a adesão, proliferação e diferenciação celular, uma vez que permitem imitar a estrutura natural da matriz extracelular.

Neste contexto, este trabalho pretende produzir biomateriais que promovam a regeneração do nervo periférico. Desta forma, desenvolveu-se as membranas de PLA com gelatina de peixe através da técnica de *electrospinning*, em cinco rácios diferentes. Além disso, o potencial destas membranas para a sua utilização na regeneração do nervo periférico foi caracterizado em termos das suas propriedades físico-químicas. As propriedades biológicas das membranas desenvolvidas foram caracterizadas através de ensaios de citotoxicidade *in vitro*. Estes estudos revelaram que as membranas produzidas pela técnica de *electrospinning* são biocompatíveis e, as membranas PG11 provaram ser um substrato adequado para promover a adesão e proliferação de fibroblastos, em comparação com o uso individual das membranas de PLA e GE, uma vez que a sua morfologia e estrutura foi melhorada.

**Palavras-chave:** *Electrospinning*, gelatina de peixe, ácido poli-láctico, regeneração do nervo periférico, engenharia de tecidos.



# Acknowledgments

Começo por agradecer aos meus orientadores, Professor José Domingos Santos e Professor Vitor Sencadas, por me terem dado a oportunidade de realizar este trabalho. Agradeço também a disponibilidade, orientação e as correções pertinentes essenciais para aumentar a qualidade deste trabalho.

Gostaria também de deixar um agradecimento à Professora Maria Helena Fernandes por me proporcionar os meios para a realização dos ensaios *in vitro* e à Liliana que me ajudou com todos os procedimentos laboratoriais.

Agradeço também às minhas amigas e ao João que sempre me ajudaram, pelos conselhos e paciência. Um especial obrigada à Raquel por saber sempre o que me dizer nos momentos mais difíceis.

Por último, um obrigada à minha família, em especial à minha mãe e às minhas irmãs que sempre me apoiaram e incentivaram durante o meu percurso académico.



# Contents

List of Figures .....	ix
List of Tables .....	xi
Abbreviations .....	xiii
Chapter 1 .....	1
Introduction .....	1
1.1 - Motivation and Context .....	1
1.2 - Objectives .....	3
1.3 - Document Structure .....	3
Chapter 2 .....	5
Literature Review .....	5
2.1 - Classification of Nervous System .....	5
2.2 - Cellular components of the PNS .....	5
2.3 - Peripheral Nerve Anatomy .....	6
2.4 - Peripheral Nerve Injuries .....	7
2.4.1- Types of Injuries .....	7
2.4.2- Wallerian Degeneration .....	9
2.5 - Treatments of Peripheral Nerve Injuries .....	10
2.6 - Tissue Engineering Nerve Grafts .....	10
2.6.1- Requirements of an ideal scaffold .....	11
2.6.1.1 - Biocompatibility .....	12
2.6.1.2 - Biodegradability .....	12
2.6.1.3 - Permeability .....	12
2.6.1.4 - Biomechanical Properties .....	13
2.6.1.5 - Surface Properties .....	13
2.6.2- Neural Scaffold Material .....	14
2.6.2.1 - Synthetic Materials .....	14
2.6.2.1.1 - Poly(Lactic Acid) .....	15
2.6.2.2 - Natural Materials .....	16
2.6.2.2.1 - Fish Gelatine .....	16

2.6.3- Methods for nanofiber processing.....	17
2.6.3.1 - Electrospinning.....	18
<b>Chapter 3 .....</b>	<b>21</b>
<b>Materials and Methods.....</b>	<b>21</b>
3.1 - Materials .....	21
3.2 - Electrospinning.....	21
3.3 - Cross-linking .....	22
3.4 - Materials Characterization .....	22
3.4.1 - Scanning electron microscopy (SEM).....	22
3.4.2 - Diameter measurements .....	22
3.4.3 - Determination of the degree of cross-linking .....	23
3.4.4 - Contact angle measurements .....	23
3.4.5 - Swelling and water retention capacity .....	23
3.4.6 - Thermogravimetric analysis .....	24
3.4.7 - Differential scanning calorimetry .....	24
3.4.8 - Fourier transform infrared spectroscopy .....	24
3.5 - Cell culture procedure.....	24
3.6 - Cell viability and proliferation .....	24
3.7 - Statistical analysis.....	25
<b>Chapter 4 .....</b>	<b>27</b>
<b>Results and Discussion.....</b>	<b>27</b>
4.1 - Morphology of the electrospun membranes.....	27
4.2 - Degree of cross-linking .....	30
4.3 - Contact angle measurements.....	31
4.4 - Swelling Degree .....	32
4.5 - Thermal behaviour .....	33
4.6 - Infrared spectra .....	36
4.7 - Cell viability and proliferation .....	38
<b>Chapter 5 .....</b>	<b>41</b>
<b>Conclusions and Future Work.....</b>	<b>41</b>
5.1 - Conclusions .....	41
5.2 - Future Work .....	42
<b>References.....</b>	<b>43</b>
<b>Appendix A .....</b>	<b>49</b>

## List of Figures

2.1	Peripheral motor neuron with its structural features: cell body and axon extension surrounded by myelin sheath produced by Schwann cells (Adapted from [21]).	6
2.2	Cross-sectional anatomy of peripheral nerve [2].	7
2.3	Schematic representation of the five grades of nerve injury according to Sunderland's classification: (1) Sunderland grade I, (2) Sunderland grade II, (3) Sunderland grade III, (4) Sunderland grade IV, (5) Sunderland grade V [8].	8
2.4	Degeneration and regeneration after peripheral injury [26].	9
2.5	The structure of nerve guidance conduits showing the sequence of events that occur in peripheral nerve regeneration [27].	11
2.6	The stereoisomers of lactic acid: L-Lactic Acid and D-Lactic Acid [35].	15
2.7	Structure of poly(lactic acid) and its degradation product, lactic acid [6].	15
2.8	Schematic diagram of the basic experimental electrospinning setup [59].	19
4.1	SEM morphologies of the electrospun polymeric nanofibers; (A) PLA, (B) PG31, (C) PG31 cross-linked, (D) PG11, (E) PG11 cross-linked, (F) PG13, (G) PG13 cross-linked, (H) GE and (I) GE cross-linked.	28
4.2	Evolution of fibre mean diameter for electrospun fibres samples before and after cross-linking; bars represent means $\pm$ SD.	29
4.3	Optical absorbance of the gelatine powder and the PLA/gelatine membranes.	30
4.4	Degree of cross-linking for gelatine and PLA/GE electrospun membranes.	31
4.5	Evolution of water contact angles for electrospun fibres membranes. Values are mean $\pm$ SD.	32
4.6	Equilibrium swelling ratio of PLA/gelatine electrospun membranes with different blending compositions.	32
4.7	a) TGA data for pure PLA and GE samples, as well as for the PLA-GE and b) DTG curves for the obtained scaffolds.	33
4.8	DSC thermograms for electrospun fibres samples.	35
4.9	FT-IR spectra for the pure PLA, pure gelatine and the PLA:GE blend membranes.	36
4.10	Resazurin viability of fibroblast cells after 1, 4, 7 and 14 days of being seeded. "PLA" cells seeded in PLA membranes; "PG31" cells seeded in PG31 membranes; "PG11" cells seeded in PG11 membranes; "PG13" cells seeded in PG13 membranes; "GE" cells seeded in gelatine	

membranes. Each result is presented as the mean  $\pm$  SD of four replicates. Statistical analysis was performed using two-way ANOVA with Dunnet's post hoc test being the significant differences when compares to control for each day (\* p<0.05). ..... **38**

**A.1** Calibration curve of BSA protein used to determine the amount of free amino groups in the sample to calculate the degree of cross-linking. .... **49**

## List of Tables

2.1	Classification of nerve injury [2,8,19,24,25].	8
2.2	Available FDA-approved nerve guide conduits [31,37].	14
3.1	Description of membranes developed according to the weight ratio of PLA and gelatine.	22
4.1	Infrared bands associated with different phases of PLA (Adapted from [13]).	37
4.2	FT-IR spectra characteristics of fish gelatine.	37



# Abbreviations

BSA	Bovine serum albumin
CBB	Coomassie Brilliant Blue G
CNS	Central Nervous System
DHT	Dehydrothermal
DNA	Deoxyribonucleic acids
DSC	Differential scanning calorimetry
DTG	Derivative thermogravimetric
ECM	Extracellular Matrix
FBS	Fetal bovine serum
FDA	Food and Drug Administration
FT-IR	Fourier transform infrared
GA	Glutaraldehyde
GE	Gelatine
HFIP	Hexafluoro-2-propanol
NGC	Nerve Guidance Conduits
NHS	N-hydrocysuccinimide
PBS	Phosphate buffered saline
PCL	Poycaprolactone
PGA	Poly(glycolic acid)
PLA	Poly(lactic acid)
PDLA	Poly(D-lactic acid)
PDLLA	Poly(D,L-lactic acid)
PLLA	Poly(L-lactic acid)
PLGA	Poly(L-lactic-co-glycolic acid)
PNS	Peripheral Nervous System
ROP	Ring-opening polymerization
SD	Standard deviation
SEM	Scanning electron microscopy
T <sub>cc</sub>	Cold-crystallization temperature
T <sub>g</sub>	Glass transition temperature
T <sub>m</sub>	Melting temperature
TGA	Thermogravimetric analysis
UV	Ultraviolet
WCA	Water angle contact
XCL	Cross-linking degree



# Chapter 1

## Introduction

### 1.1 - Motivation and Context

Injuries to the peripheral nervous system (PNS) are a major cause for permanent disabilities with a strong effect on a diminished quality of life. The neurological sequels left by this kind of injuries result in a diminished daily live activity as well as loss of work capabilities.

Peripheral nerve injuries are the principal cause of disorders with devastating impact on quality of life of patients. Neurological sequels caused by this kind of injuries compromise the daily activities and work skills. Therefore, this has a socioeconomic impact. The main symptoms of these injuries result in motor and sensory functions loss, which result in complete paralysis of the affected limbs or the development of neuropathic pain [1-5]. PNS injuries are classified according to its origin in traumatic, non-traumatic and surgical.

Traumatic peripheral nerve injuries result from collisions, motor vehicle accidents, gunshots wounds, fractures or lacerations. Non-traumatic injuries are attributed to nerve compression and adhesion. Surgical nerve injuries result from procedures to remove prostate tumours [6]. This kind of injuries affects a large part of the population over the world. It is estimated that about 2.8% of trauma patients, many of whom acquire life-long disability, are affected by peripheral nerve injuries. In Europe, over 300,000 cases of peripheral nerve injury occur annually [7] and 200,000 people in the United States suffer from peripheral nerve injury caused by trauma and medical disorders [5]. That is the main reason why the surgery to repair the damage to the peripheral nerve is urgently needed as well as a medical challenge [7].

Experimental work has been done that reveals the existence of neurobiological activity crucial to the regeneration of the peripheral nerve and target reinnervation [1]. Unlike what happens in the central nervous system (CNS), the peripheral nervous system has an intrinsic ability for repair and regeneration under proper conditions [3, 7]. This is mainly due to differences in response to injury of glial cells. The Schwann cells, glial cells of the PNS, convert to a regenerative phenotype thereby promoting the formation of a basal lamina and providing abundant cues to trigger neuronal regenerative response [3].

However, the capacity for regeneration depends on many factors including the time elapsed, type of injury, patient's age and in particular to the proximity of the injury to the nerve cell body [3,5].

In fact, there is an acceptable period of approximately 12-18 months for muscles reinnervation to occur in order to achieve functional recovery before irreversible motor end plate degeneration follows [2,8]. The axonal regeneration rate, in humans, is slow around 1-2 mm/day. Thus, for severe injuries may take many months to heal [2].

In recent years, various surgical techniques have been carried out to aid the regeneration and repair of damage in peripheral nerves [7]. However, the functional recovery is usually incomplete [1,4,9]. The combination of slow axonal regeneration, structural changes in muscle targets and an increasingly less supportive stromal environment for regeneration all contribute to an incomplete recovery [2].

Thus, a promising alternative is to use natural and synthetic neural scaffolds in which tubular nerve guidance conduits (NGC) is the basic structure. This approach is denominated tubulization. The mechanism of using a nerve guide for the regeneration of a damaged peripheral nerve is that a gap is left between the nerve stumps sutured into either end of the tube. Guidance channels provide a microenvironment and mechanical support, directing the axonal growth from the proximal to the distal nerve stumps, while neuroma formation and ingrowth of fibrous tissue into the nerve gap is prevented [5, 9, 10-11]. In addition, they are designed and fabricated to increase the number, speed and length of the regenerating nerves [5].

A very important factor for the fabrication of NGC is the biomaterials selection [7,11]. That is the main reason why different types of biologic and artificial grafts have been developed and investigated in their regeneration capacity and functional recovery [7, 12]. Natural biomaterials are extremely useful in tissue engineering, especially in nerve regeneration, because they stimulate adhesion, migration, growth and proliferation of cells and have good biocompatibility [4]. Synthetic materials constitute another class of promising biomaterials due to their physiochemical and biological properties that can be specifically tailored to match different application requirements, rate degradation in a good time span, and the degradation products are easily absorbed by the body [7,10].

The structure of neural scaffold is an important factor that determines the effectiveness of the scaffold for peripheral nerve regeneration. The neural scaffold can be manufactured in its basic structure, i.e., the tubular NGC with a single hollow lumen. However, modifications have been developed to create a more complex structure, where the NGC lumen has an intricate internal architecture, where physical fillers are introduced into the lumen NGC. To enhance peripheral nerve regeneration, fibres were successfully used as intraluminal fillers [5,7].

In addition to the material selection, fabrication methods are also critical for designing neural scaffolds [6]. Nanofibers can be produced by diverse manufacturing methods, such as drawing, electrospinning, phase separation, self-assembly, template synthesis and wet spinning [13-15]. However, electrospinning has proven to be an excellent method for the synthesis of thin fibres to build three-dimensional tissue engineering scaffolds [6,13]. Nanofibers scaffolds served as suitable environment for cell attachment, proliferation and differentiation because they can potentially mimic the structure of natural extracellular matrix (ECM) [6, 14,16-17].

## 1.2 - Objectives

This study will focus on the development and characterization of fibrous membranes, produced through the electrospinning technique, of poly(lactic acid) (PLA) blended with fish gelatine (GE). The potential of these membranes for peripheral nerve regeneration will be characterized in terms of their physical, chemical and mechanical properties and biological performance. This study intends to assess membranes cytotoxicity and verify if they are responsible for accelerating axonal regeneration process in order to promote the reinnervation and improve the functional recovery.

## 1.3 - Document Structure

The report is divided in 5 chapters. The motivation and objectives have already been described in this first chapter. In Chapter 2, the contextualization of key aspects is presented, particularly the classification and anatomy of nervous system, types of injuries, the current treatments of peripheral nerve injuries. Chapter 3 is relative to the materials and methods and Chapter 4 to the obtained experimental results and its discussion. Finally, Chapter 5 summarizes the main conclusions of this research and discusses future work.



# Chapter 2

## Literature Review

In this chapter is presented the contextualization of the principal biological aspects relevant for this report. Initially, the classification and anatomy of nervous system will be presented. Additionally, the types of injuries will be described, followed by the events that occur after these injuries. Finally, the current treatments of peripheral nerve injuries will be explained, with particularly focus on nerve grafts and the production techniques of these grafts.

### 2.1 - Classification of Nervous System

The nervous system is structurally divided into the central nervous system (CNS) and peripheral nervous system (PNS). The CNS consists of the brain and the spinal cord. The PNS includes all the nervous tissue outside the CNS, such as sensory receptors, nerves, ganglia, and plexuses. Neurons in the PNS are classified according to the direction in which the neuron conducts the nervous impulse. Sensory or afferent nerves transmit electrical signals, known as action potentials, from the sensory receptors to the CNS and motor or efferent nerves conduct electrical signals from the CNS to effector tissues, such as muscles and glands. Motor neurons are also divided as somatic and automatic [2,10,18].

### 2.2 - Cellular components of the PNS

The two types of cells that comprise the nervous system are neurons and neuroglia or glial cells.

Neuroglia are non-neural cells that support and protect neurons. The glial cells of the PNS are Schwann cells and satellite cells [18]. Schwann cells forms a myelin sheath at regular intervals that allow faster and more intense propagation of signals along the axon. In addition, Schwann cells have an important role in maintaining normal nerve function and in mediating nerve repair following injury. The myelin sheath is not continuous but is interrupted. These interruptions are the nodes of Ranvier, which initiate and propagate action potentials [18-20]. The basal lamina that surrounds the Schwann cells and the associated axon is produced by the

Schwann cells. Extracellular matrix molecules in the basal lamina, such as laminin and collagen, regulate the formation, architecture and function of myelin [20].

The neuron (Figure 2.1), or nerve cell, is the functional unit of the nervous system and is an electrically excitable cell that process and transmits information by electrical and chemical signalling. Neurons are characterized by a cell body and two types of cellular projections, called dendrites and axons. The cell body, or soma, contains a single nucleus. Dendrites are short extensions of the neuron cell body. Dendrites usually receive information from other neurons or sensory receptors and transmit electrical signals to the cell body. An axon is a single long cytoplasmic process extending from the cell body. Axons conduct electrical impulses away from the cell body. Axons in the PNS are surrounded by a highly specialized layer of Schwann cells called the myelin sheath. This characteristic proves to be significant in terms of regeneration [10,18].

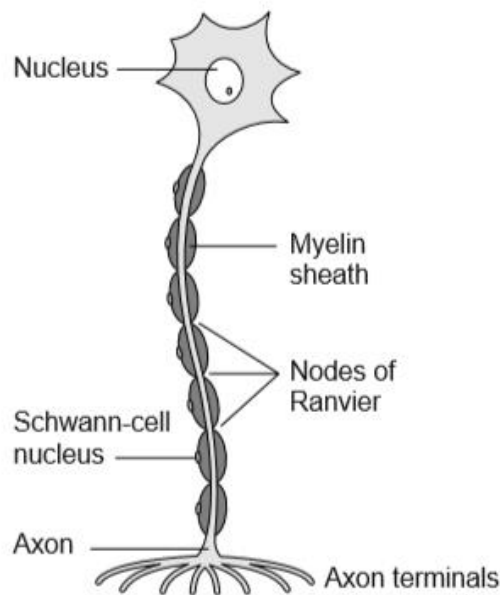


**Figure 2.1** - Peripheral motor neuron with its structural features: cell body and axon extension surrounded by myelin sheath produced by Schwann cells (Adapted from [21]).

### 2.3 - Peripheral Nerve Anatomy

A nerve (Figure 2.2) is a bundle of motor and sensory axons that are grouped together by supportive tissue into an anatomically defined trunk. There are four types of collagen-containing connective tissue that provide structure to the nerve fibres: endoneurium, perineurium, epineurium and mesoneurium. Endoneurium surrounds an individual axons and their Schwann cells sheath and it is composed of thin oriented collagen fibres and some fibroblasts. Axons and their associated endoneurium are grouped together to form small bundles called fascicles. The perineurium, formed from multiple layers of perineural cells and collagen, surrounds these fascicles. The perineural cells provide a barrier between the nerve and its blood supply, while the collagen provides the nerve's tensile strength. Many fascicles are arranged in large bundles, which are surrounded by a connective tissue layer called the epineurium. The internal epineurium separates fascicles while the external epineurium

surrounds many fascicles and defines the nerve anatomically. Finally, external to this layer is the mesoneurium, containing the blood supply to the nerve [2,8,10,19].

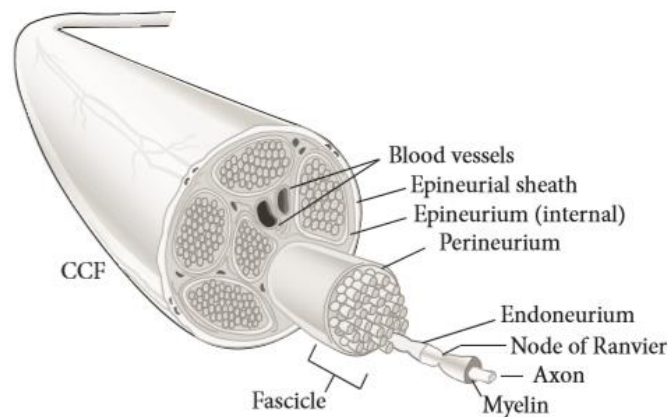


Figure 2.2 - Cross-sectional anatomy of peripheral nerve [2].

## 2.4 - Peripheral Nerve Injuries

### 2.4.1 - Types of Injuries

Peripheral nerve injuries can result from chemical, mechanical, pathological and thermal damage [10]. Two classifications for peripheral nerve injuries have been proposed by Seddon and Sunderland [2]. In 1943, Seddon described three types of nerve injury: neurapraxia, axonotmesis and neurotmesis (Figure 2.3) [22].

Neurapraxia is the mildest type of nerve injury and refers to a temporary interruption of nervous conduction, without disruption of the axon or perineurium. However, since the basic structure of the axon is preserved, Wallerian degeneration does not occur [19,23]. Clinically, it results in sensory dysfunction [24]. These injuries typically lead to complete recovery within 12 weeks once myelination is restored [2].

Axonotmesis refers to loss of axonal continuity while the connective tissue layers are preserved. Since the axon is disrupted, Wallerian degeneration occurs. Incomplete recovery is common, depending on the degree of internal disorganization and the distance between the injury and target tissue [2,8,24].

Neurotmesis is the most severe nerve injury with complete transection of both axons and connective tissue. There is a total loss of motor and sensory function. After neurotmesis, spontaneous regeneration does not occur in absence of surgical intervention [2,22-23].

In 1951, Sunderland expanded the classification based on histology to include five categories: type I to type V [2].

Sunderland first degree corresponds to neurapraxia. The second, third and fourth degrees are equivalent to axonotmesis. This classification adds two useful subclasses of axonotmesis. Finally, fifth degree are termed neurotmesis [2,8,25].

Second degree injuries have axonal damage without breaching the connective tissue of the fibres. In third degree injuries, the axon and the endoneurium are disrupted, although the

perineurium is preserved. In fourth degree injuries, the endoneurium and perineurium are disrupted [8,19,25]. Sunderland type I and II recover completely, type III recovers partially and type IV and V require surgical intervention [2].

Table 2.1 - Classification of nerve injury [2,8,19,24,25].

Seddon	Sunderland	Affected structure(s)	Recovery
Neurapraxia	Type I	Myelin	Complete
Axonotmesis	Type II	Axon	Complete
Axonotmesis	Type III	Axon, endoneurium	Partial
Axonotmesis	Type IV	Axon, endoneurium, perineurium	Surgical intervention required
Neurotmesis	Type V	Axon, endoneurium, perineurium, epineurium	Surgical intervention required

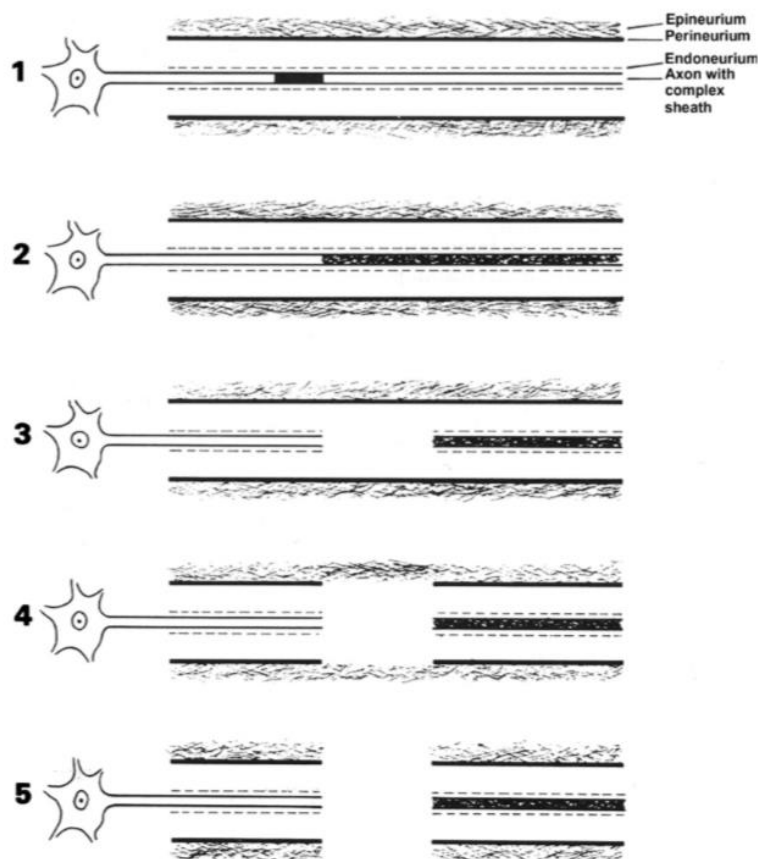


Figure 2.3 - Schematic representation of the five grades of nerve injury according to Sunderland's classification: (1) Sunderland grade I, (2) Sunderland grade II, (3) Sunderland grade III, (4) Sunderland grade IV, (5) Sunderland grade V [8].

### 2.4.2 - Wallerian Degeneration

Once a peripheral nerve has been transected, a series of molecular and cellular events, known as Wallerian degeneration, occurs in the distal stump of the injured nerve and within a small zone distal to the proximal stump. This starts the disintegration of the axoplasmic microtubules and neurofilaments [4,7]. Within a few hours, both axons and myelin in the distal stump of the transected nerve are transformed in granular and amorphous debris by the Schwann cells. In the proximal stump, degeneration also occurs back to the adjacent node of Ranvier, the site of subsequent axonal regrowth. Then macrophages and monocytes migrate to the area of injury releasing growth factors, which stimulate Schwann cell and fibroblasts proliferation [2,7].

When the debris has been removed, Schwann cells proliferate to form longitudinal cell columns, called Bands of Bungner, within the basal lamina of the denervated distal endoneurial tubes [3,20]. Schwann cells also begin to secrete neurotrophic factors and extracellular matrix molecules that stimulate the regeneration, which starts at the proximal stump and continues toward the distal stump. This environment is crucial for successful peripheral nerve regeneration [3-4,7].

The new axons sprout from the most distal node of Ranvier and are remyelinated by Schwann cells. In order to get a functional reinnervation it is necessary that the regenerating axons elongate under the mediation of growth cones until they connect with a receptor. However, sometimes the synaptic target is not reached. When it happens, growth cone branches continue to grow in a disordered manner forming a neuroma (Figure 2.4-E), which result in phantom limb and neuropathic pain [2,7,10].

The axonal regeneration rate, in humans, is slow around 1-2 mm/day. Thus, for severe injuries may take many months to heal [2].

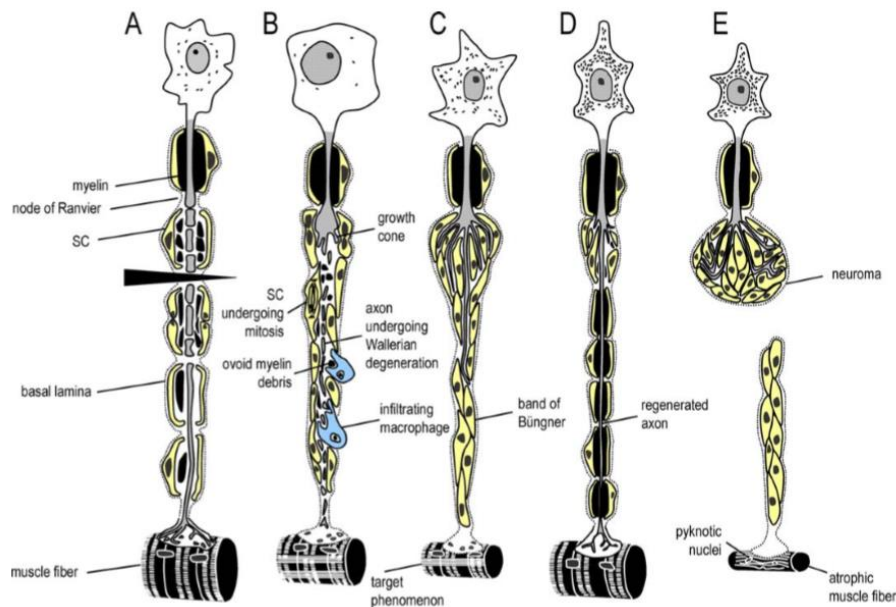


Figure 2.4 - Degeneration and regeneration after peripheral injury [26].

## 2.5 - Treatments of Peripheral Nerve Injuries

In order to repair these nerve injuries, several techniques have been used [6]. Currently, two surgical techniques are used to regenerate the peripheral nerve: manipulative nerve operations and bridge operation. The manipulative surgeries include direct neurorrhaphy and nerve transfers. These techniques are performed when there was no significant loss of nerve tissue and it is possible approximation with minimal tension [5,7].

Neurorrhaphy is the surgical suturing of a divided nerve through end-to-end or end-to-site coaptations. This method is limited to the treatment of short defects because the fascicular coaptation may cause excessive tension between both nerve stumps, which would inhibit nerve regeneration [4-5,7]. During this process, the correct alignment of the nerve fascicles is crucial in successful regeneration [27].

Nerve transfers or neurotization are basically the transfer of nerve sections of other healthy nerves, with not so important functions, to the damaged nerves considering that their function is much more important [5,7].

The bridge operations include grafting, transposition and tubulization techniques [7].

In cases where loss of nerve segment is substantial resulting in a gap, where tension-free neurorrhaphy is not possible, the interposition of a nerve graft, as a bridge, between the proximal and distal nerve stumps is often necessary [3-4,7].

Usually, the typical choice is to use an autologous nerve graft from some less important part of the body [7]. Nerve autografts are the current gold standard method to repair nerve gaps [5]. This technique provides structural support to guide axonal regeneration, preventing neuroma formation and fibrous tissue invasion [3]. However, there are several disadvantages with this technique including the limited availability of donor nerves, the need for a second surgery to obtain de donor nerve, donor site morbidity that may include the possibility of painful neuroma, scaring and sensory loss [4-5,7,10].

These problems drive the search of different solutions to supplement or substitute autologous nerve grafts [7]. The use of neural scaffolds to bridge nerve gaps is a promising alternative, and this approach is denominated tubulization [5,7].

## 2.6 - Tissue Engineering Nerve Grafts

The use of neural scaffolds involves two interrelated aspects, the scaffold configuration and scaffold fabrication [3]. The neural scaffolds can be prepared with different structures, in which tubular nerve guidance conduit (NGC) is the basic structure [4,7].

The mechanism of using nerve guidance conduits for the regeneration of a damaged peripheral nerve is that a gap is left between the nerve stumps sutured into either end of the tube [10-11].

Neural scaffolds serve to direct axons sprouting from the proximal to distal nerve stumps [10-11,28], keep the adequate mechanical support to the regeneration of nerve fibres [5,7], provide a conduit channel for the diffusion of neurotropic and neurotrophic factors secreted by the damage nerve stump, as well as the interface for the exchange of nutrients and residual products, prevent the infiltration of fibrous tissue and neuroma formation that disable the axonal regeneration [7,10-11,28], provide an optimal microenvironment for the regeneration of the nerves increasing the concentration of endogenous proteins [7,10]. Furthermore, that

they must be easy to produce, sterilize and implant in the body with microsurgical techniques [7].

In addition, they are designed and fabricated to stimulate the regeneration process actively increasing the number, speed and length of regenerating nerves [5,10].

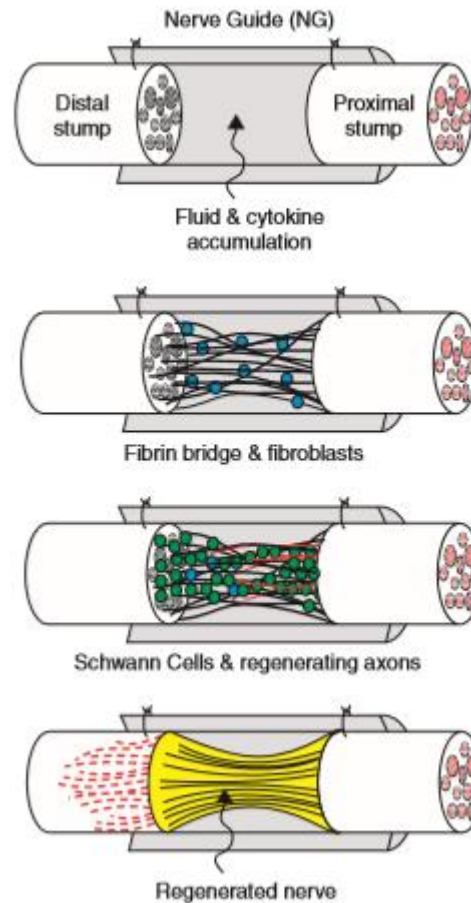


**Figure 2.5** - The structure of nerve guidance conduits showing the sequence of events that occur in peripheral nerve regeneration [27].

Thus, in addition to the requirements listed above, other important properties must be considered.

### 2.6.1 - Requirements of an ideal scaffold

The properties determined by the scaffold material and its structure, are the most important to satisfy many physical and biologic requirements of each scaffold, along with biocompatibility, biodegradability, permeability, biomechanical and surface properties [7,29].

### 2.6.1.1 - Biocompatibility

The first criteria to be taken into consideration is the biocompatibility and function without interrupting other physiological process. The scaffold must be able to work as a substrate that supports the appropriate cellular behaviours, such as promotion of molecular and mechanical signalling systems to help nerve regeneration [7,14]. The cells should adhere and migrate to the surface and eventually proliferate before a new matrix is formed [15,30]. In addition, after implantation, the scaffold must not promote or initiate any undesirable effects on neural cells and tissues or eliciting any undesirable local or systemic responses in the neural scaffold, in order to avoid the rejection of the scaffold by the body [7,14]. The biocompatibility of the scaffolds is affected by the polymer synthesis, scaffold processing and sterilization conditions [14].

The biocompatibility of neural scaffolds can be measured from three different aspects: blood and mechanical compatibility and histocompatibility. In order to have a good blood biocompatibility it is required that the scaffold in contact with the blood does not induce hemolysis, destroy blood components, or lead to coagulation and thrombus formation. Histocompatibility means that the scaffold has no toxic side effects on the surrounding tissue, while the last ones do not induce corrosive effects or immune rejection of the scaffold. Finally, mechanical compatibility refers to the matching of mechanical properties between the scaffold and nerve tissue [7].

### 2.6.1.2 - Biodegradability

Biodegradability is a very important property that has a very special task on the tissue regeneration. The scaffold should be able to degenerate or be resorbed *in vivo* allowing the body to replace the scaffold with its own cells. In fact, scaffolds are not made to be used as replacements but as support for a new cell structure [10,12,30]. Scaffold degradation occur through physical, chemical or biological processes that are mediated by biological agents, such as enzymes in tissue remodelling [14]. The degradation products must be non-toxic and be expelled from the body with any interference with any other organs [30].

During nerve regeneration, neural scaffolds must be able to cope with some mechanical stress from neighbouring tissues and maintain at least a slight elasticity and bendability without collapse or losing their shape [7]. On the other hand, the degradation rate should be tuned to match the regeneration rate of the nerve [7,14].

The scaffold biodegradation rate depends on the properties of the polymer, including the chemical structure, the wettability, morphology, glass transition temperatures and the molecular weight [14].

### 2.6.1.3 - Permeability

A neural scaffold must have the adequate permeability to allow the nutrients, gas and metabolic waste exchange, including the exchange of fluids between the regeneration environment and surrounding tissues, through pores in the conduit wall [7,31].

Also, permeability may be needed for the viability of supportive cells [32], since the porous structure provide a large surface area that will allow cell ingrowth, uniform cell distribution,

and facilitate the revascularization of the neural guidance conduit [14]. However, pore size is also a very important issue because the pores should be small enough to prevent fibrous scar tissue invasion [9]. It is also important for the formation of the fibrin matrix during the first period of nerve regeneration [7,31-32].

There are different fabrication techniques through which neural scaffolds can be made permeable, such as cutting holes into the wall, rolling of meshes, fibre spinning, adding pore-formation agent or injection-molding followed by solvent evaporation. In addition, the hydrophilic property of the scaffold material is a critical factor and is responsible for the permeability of the neural scaffold [7,32].

#### 2.6.1.4 - Biomechanical Properties

Mechanical strength is one of the properties that must be analysed. The scaffold should have proper mechanical properties to encourage the rapid regeneration of the tissue [14] and maintain a stable support structure for nerve regeneration [9]. Scaffolds must have Young modulus close to the tissues where it will be implanted, in order to resist *in vivo* physiological loads during nerve regeneration. To meet this basic requirements, the biomedical parameters of native peripheral nerves have been determined. It is accepted that Young's modulus of peripheral nerves in the longitudinal direction is 0.50 MPa and the ultimate load of human ulnar or median nerve is 65-155 and 72-220 N, respectively [7]. In other words, the tube should be able to resist compression, but be flexible enough to prevent mechanical irritation [33]. Thus, a balance should be found between flexibility and rigidity, because if the scaffolds is too rigid some dislocation can result but if is too flexible, the axonal regeneration can be failed [4,7].

In order to control the mechanical strength of nerve guidance conduits, several approaches have been taken such as cross-linking, coil-reinforcement and tuning the material composition. In addition, the degree of cross-linking also offers a mechanism to tune the degradation rate of the nerve conduits [28].

#### 2.6.1.5 - Surface Properties

Surface properties, including chemical and topographical characteristics, are important in the interaction between the scaffold and nerve cells because the scaffold surface is the initial site of interaction with the surrounding cells and tissue [7]. The longitudinally oriented surface texture is thought to mimic the endoneurial tubules naturally found in nerves, which has been shown to influence directional outgrowth of axons and uniform alignment of Schwann cells *in vitro*, and improved nerve regeneration *in vivo* [7,28].

The incorporation of physical fillers in the lumen to form an internal matrix was the more important modification to the basic structure of neural scaffolds because the matrices attempt to increase the bioactivity of NGC and prevent their collapse [28].

Scaffolds with a high internal surface-area-to-volume ratio is essential in order to accommodate the number of cells required to replace or restore tissue functions [14]. The use of nanofibrous scaffolds offer optimal surface properties because these scaffolds mimic the topography of natural ECM and provide a high surface area for cell attachment and growth and topographic signals favourable for directing cellular functions [34]. In addition, the introduction of fibres into the NGC lumen also increase the overall cross-section area of regenerated nerve

tissues, enhances the formation of myelinated axons, and promotes the sensory functional recovery [7].

## 2.6.2 - Neural Scaffold Material

One of the most sensitive steps with respect to the tissue engineering process consists on the choice of biomaterials with the desired features to be used as scaffolds. The criteria for selecting the materials is based on their material chemistry, molecular weight, solubility, shape and structure, wettability, surface energy and degradability [14].

Polymer materials have received great attention and have been widely used in tissue engineering because their properties can be tailored [35] and are inexpensive [36]. Polymeric scaffolds can be synthetic or natural.

Currently, the available FDA-approved nerve conduits are: NeuraGen, Neuroflex, Neuromatrix, Neurawrap, Neuromend, Neurotube, Neurolac and Salutunnel. These nerve conduits have similar structure but the composition is different. However, these nerve conduits only can be used for short nerve gaps [31,37].

**Table 2.2** – Available FDA-approved nerve guide conduits [31,37].

Product Name	Material
NeuraGen	Collagen Type I
NeuroFlex	Collagen Type I
NeuroMatrix	Collagen Type I
NeuraWrap	Collagen Type I
NeuroMend	Collagen Type I
Neurotube	Polyglycolic acid (PGA)
Neurolac	Poly(DL-lactide- $\epsilon$ -caprolactone) (PLC)
SaluTunnel	Polyvinyl Alcohol (PVA)

### 2.6.2.1 - Synthetic Materials

The use of biodegradable synthetic materials in neural scaffolds has shown promising results, with degradation rate in a good time span and the resulting products being easily absorbed by the body [7]. Moreover, they can be tailored mechanically, chemically and biochemically to suit various applications [11].

Among the biopolymers, the groups of poly( $\alpha$ -hydroxy acids), including poly(lactic acid) (PLA), poly(glycolic acid) (PGA), polycaprolactone (PCL) and their copolymers, such as poly(lactic acid- $\epsilon$ -caprolactone), poly(L-lactic-co-glycolic acid) (PLGA) e poly(1,3-trimethylenecarbonate- $\epsilon$ -caprolactone), all of them approved by the Food and Drug Administration (FDA) in the United States for use as biomaterials, are the most widely used synthetic biodegradable materials to replace and support damaged tissue [6,7,31].

### 2.6.2.1.1 - Poly(Lactic Acid)

PLA is known to be one of the most commonly used biomaterials [12], due to its four attractive advantages, such as renewability, biocompatibility and processability and mechanical properties [35,38]. PLA is obtained by the processing and polymerization of lactic acid monomer (2-hydroxypropionic acid) [39] and is derived from renewable and degradable sources such as corn, rice and sugar cane [40]. Currently, the polymerization processes used to prepare PLA are direct polycondensation and ring-opening polymerization (ROP) [39].

PLA is an aliphatic polyester that exists in the form of two stereoisomers (Figure 2.6): poly(L- lactic acid) (PLLA) and poly(D-lactic acid) (PDLA) and the mixture of both components is poly(D,L-lactic acid) (PDLLA) [13]. PLLA and PDLA are semi crystalline materials with a regular chain structure, whereas PDLLA is amorphous [35]. PLLA is the mainly used form in biomedical applications, because the degradation product L-lactic acid is the natural occurring stereoisomer of lactic acid [11].

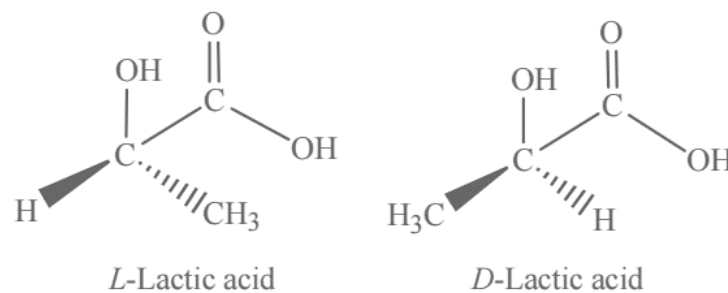


Figure 2.6 - The stereoisomers of lactic acid: L-Lactic Acid and D-Lactic Acid [35].

The ratio of the D- or L-enantiomers and molecular weight affects PLA properties, such as mechanical strength, degree of crystallinity and melting temperature [13,40].

In fact, the most attractive aspect of PLA, especially with respect to medical field, is its biocompatibility [38]. Its degradation products are non-toxic, because lactic acid is produced in mammalian muscles during glycogenolysis and is involved in the Krebs's cycle through pyruvic acid and Acetyl-CoA [41].

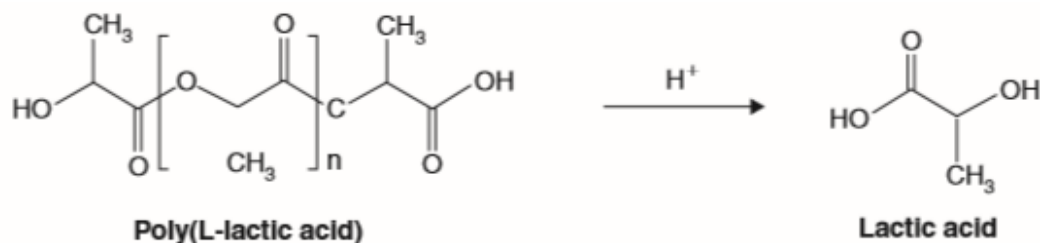


Figure 2.7 - Structure of poly(lactic acid) and its degradation product, lactic acid [6].

Apart from the properties mentioned above, PLA also exhibits a low density, low processing power, elastomeric behaviour, corrosion resistance and versatile fabrication processes [13].

Although PLA can be considered a biomaterial with excellent properties, it has some drawbacks which limit its use in certain applications. PLA has a degradation rate slow, poor ductility [35] and is strongly hydrophobic, which limits cell attachment, viability and proliferation [42].

In order to overcome this problem, many strategies have been intensively investigated to improve the biocompatibility of PLA [42]. Blending synthetic and natural polymers, such as gelatine, is a feasible approach to achieve the desired behaviour [39].

### **Piezoelectricity**

The use of PLA is not based solely on these properties, but also due to their piezoelectric properties.

As it is possible to find electrical activity and even piezoelectricity in many parts of the body, such as bone, tendon, ligaments, cartilage, skin, dentin, collagen, deoxyribonucleic acids (DNA) and cell membranes, the use of biomaterial with piezoelectric properties is an advantageous approach [43].

In order to promote axon growth, it was found that the application of electrical stimulation in peripheral nerves immediately after axotomy can reinforce the intrinsic injury signalling mechanisms and produce a better regenerative response [1,4]. Furthermore, research has showed that electrical charges play a significant role on the proliferation and differentiation of various cell types, including neurons [10]. Hence, the use of a biomaterial scaffold that is electrically conductive may improve regeneration and functional recovery following injury, since the electrical stimulation influence the rate, orientation, extension and direction of the neurite outgrowth [44,43].

This can be achieved without the need for an external power source through the use of piezoelectric materials [45]. These materials generate transient electrical response when a mechanical stress is applied, or vice versa. As a result, piezoelectric materials provide an electrical or mechanical stimuli to the cells [58]. The electricity is generated through the deformation in the asymmetric shift of ions or charges in piezoelectric material which induces a change in the electric polarization [45].

PLA has a piezoelectric constant approximately of 10 pC/N. Therefore, its application in nerve regeneration is promising, since this material can induce electroactivity when it is mechanically deformed, providing the necessary stimuli for proper regeneration [40].

### **2.6.2.2 - Natural Materials**

Natural biomaterials have been extensively used for tissue engineering since they have advantages over synthetic materials, as similarity with natural ECM [5]. Among the natural polymers used, gelatine represent one of the most widely used, either alone or in blends with other polymers [46].

#### **2.6.2.2.1 - Fish Gelatine**

Gelatine is a biodegradable, biocompatible, non-toxic and non-carcinogenic protein [47], derived from partial hydrolysis of collagen, which is the most abundant structural protein

contained in animal bones, skin, tendons and cartilage [46] and one of the most important constituents of ECMs [48].

Gelatine is derived from mammalian sources, such as porcine and bovine, and fish. However, fish gelatine has gained great interest in compassion with mammalian due to public health reasons, such as the transmission of bovine spongiform encephalopathy or other diseases, and religious interdictions to the consumption of certain animal sources [46,49].

Due to its biological origin, gelatine is a very good material for tissue engineering application once it promotes cell differentiation, proliferation and adhesion [50].

However, the poor mechanical properties and water solubility have restricted the application of gelatine as scaffold [48]. In order to overcome the quickly dissolution in aqueous environments, but also the weak mechanical properties, cross-linking of gelatine is necessary [46]. This can be achieved either using physical methods, such as dehydrothermal (DHT) treatment and ultraviolet or gamma irradiation, or chemical methods [47] which typically use chemicals agents like aldehydes, which interact with the functional groups of proteins [51]. Several chemical substances have been applied to cross-link gelatine, such as glutaraldehyde (GA), genipin and EDC/N-hydrocysuccinimide (NHS) [47]. Amongst the cross-linking agents, GA is the most widely used because it reacts rapidly with amine groups in gelatine [49] and its vapour phase is efficient and fast in stabilizing collagenous materials [46]. The reaction occurs between the free amine groups of lysine or hydroxylysine amino acid residues in the gelatine polypeptide chains and the aldehyde groups of GA to produce imine linkages [46]. However, if released into the host due to biodegradation, GA is toxic, and poses a risk for biocompatibility [52]. The risk of cytotoxicity can be reduced by decreasing the concentration of GA solutions or through treatment to remove unreacted GA left in the material after the cross-linking treatment [53].

The introduction of gelatine in PLA matrices is expected to improve the hydrophilicity and cellular affinity. On the other hand, the poor mechanical properties of the gelatine will also be improved due to the introduction of PLA [14]. For those reasons, blending natural and synthetic polymers is a viable approach to circumvent the limitations of each material. It allows the manufacturing of new biomaterials with good cell adhesion and mechanical properties for tissue engineering applications [48].

### 2.6.3 - Methods for nanofiber processing

As mentioned before, an array of biomaterial-based fillers with different physical forms, such as fibres, are included into the single hollow lumen of the NGC to promote attachment, proliferation, migration of Schwann cells and, hence, enhance peripheral nerve regeneration. Furthermore, the biopolymer properties are also determined by the fabrication technique [7].

Nanofibers can be produced by a number of techniques such as drawing, electrospinning, phase separation, self-assembly, template synthesis and wet spinning [36].

Nanofibers have been fabricated through drawing process. In this simple technique, nanofibers were fabricated directly when a micropipette with a diameter with few micrometres was placed in a polymer solution and moved up forming a thin filament which is then solidified to form a nanofiber. However, this technique only allows the production of a single fibre at one time, i.e., has a low productivity [36,54].

Nanofibers can be fabricated using templates using templates. The major drawback of template synthesis technique is the limitation on fibre dimensions and arrangement [54].

Phase separation has been used to create porous polymers membranes. The main mechanism of this technique is the separation of phases due to physical incompatibility. This fabrication procedure involves the dissolution of polymer, polymer gelation, solvent extraction, freezing and free-drying [36,54]. Phase separation is a relatively simple procedure that does not require many specialized equipment. It is also easy to achieve batch-to-batch consistency, and mechanical properties of the matrix can be tailored by varying polymer concentrations. However, this technique is specific to certain polymers [15].

Self-assembly involves the molecule organization and arrangement into patterns or stable structures through non-covalent forces, such as hydrogen bonding, hydrophobic forces, and electrostatic reactions. This technique generally creates small nanofibers, similar with the natural ECM scale. Despite these characteristics, this technique involves a complex procedure that is limited to specific polymer configurations [15,36,54].

### 2.6.3.1 - Electrospinning

Electrospinning has proved to be one of the best methods for the synthesis of thin fibres in the order of few nanometres with small pores and large surface areas, ease of functionalisation purposes and superior mechanical properties, for a varied range of polymeric solutions [13,55].

Moreover, this technique allows the production of nanofibrous scaffolds that can mimic the structure of the fibres in natural extracellular matrix [55] at the nanometre scale (3-5000 nm) [56]. The native ECM of human tissues and organs provide support to cells and it is composed of a network of micro- and nano-scaled protein and glycosaminoglycan fibres [56]. Due to the similar architecture of the native ECM, electrospun nanofibers have been used in biomedical application, such as nerve, cartilage, bone and heart regeneration [40].

Another attractive characteristic of electrospinning process is a simple and inexpensive setup. When used in its simplest form, the setup (Figure 2.8) consists of a pipette or a syringe filled with polymer solution, a high voltage power supply and a grounded conductive collector [57].

During the electrospinning process, a high voltage (5-15 kV) is applied between a grounded collector and a positively charged needle capillary filled with a polymer solution [56]. When charges within the polymer solution reach a critical amount, i.e., the electrostatic charges overcome the surface tension of the polymer solution, a polymer jet is created and, then, it is distorted into a conical shape, resulting in the formation of the Taylor cone [36,58]. As the jet is charged electrically, the jet is subjected to a stretching process. The continuously elongation and the solvent evaporation leads to formation of an extreme thin polymer fibres [56]. The electrospinning jet moves to the region with less potential, which generally is a grounded collector, where are deposited. In the end, the fibres are collected from the collector as a web of fibres [36].

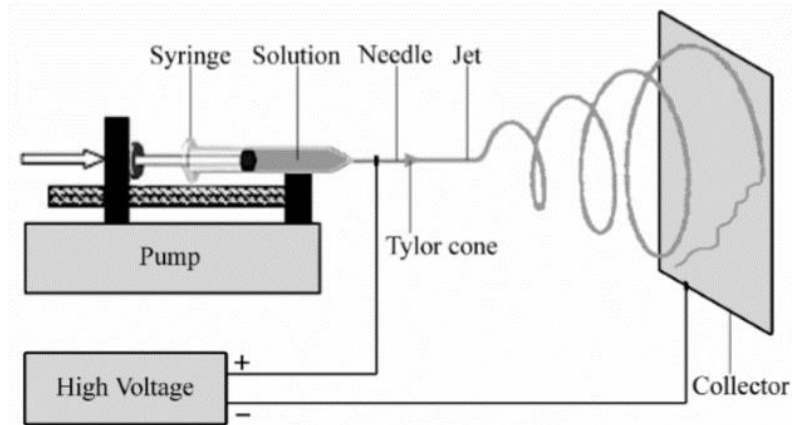


Figure 2.8 - Schematic diagram of the basic experimental electrospinning setup [59].

There are several parameters which influence the morphology of the electrospun fibres. Therefore, the knowledge of the parameters that influence the polymer solution is of great importance, in particular the molecular weight, solution viscosity, surface tension, solution conductivity and dielectric constant. Furthermore, it is also necessary to know the processing conditions which will also influence the electrospinning process, such as applied voltage, feedrate, temperature, effect of collector, needle diameter and distance from the tip to the collector. Finally, the environmental parameters, such as humidity, type of atmosphere and pressure, also affect the morphology of the fibres [13,15,36].

Although the morphology of the nanofibers can be controlled, the basic process of electrospinning only allows the formation of randomly aligned nanofibers. The alignment of nanofibers is achieved through the use of different collectors, such as a rotating cylinder collector, a rotating disk collector and two parallel conducting collectors [36]. *In vivo*, aligned electrospun fibres promoted significantly enhanced axon regeneration compared to randomly aligned electrospun fibres [36,44].

Most of the polymers are dissolved in some solvents before electrospinning, and when they are completely dissolved, they form the polymer solution. The characteristics of the solvent, such as volatility and polarity, have important effects on the morphology and diameter of the fibres. The solvent must not only dissolve the polymer, but also evaporate within the distance between the tip and the collector. This can be achieved with solvents like dimethylformamide, tetrahydrofuran and hexafluoro-2-propanol (HFIP) [58]. However, the HFIP has low surface tension which allows the production of fibres with a smaller average diameter. For these reasons, PLA, gelatine and PLA/gelatine fibres are produced by electrospinning, dissolving the polymer solution in HFIP [50].



# Chapter 3

## Materials and Methods

This section outlines all the experimental work performed. The objectives established for this work were to prepare novel polymeric blends between natural and synthetic polymers and evaluate the potential of PLA/gelatine membranes for peripheral nerve regeneration. In this way, their physical, chemical and mechanical properties and biological performance were assessed. Thus, this work is divided into three main steps: development and characterization of membranes, *in vitro* evaluation.

### 3.1 - Materials

Poly(L-lactic acid) (PLA, Purasorb PL18, from Corbion), fish gelatine (GE, from Sigma-Aldrich) and hexafluoroisopropanol (HFIP, analytical grade > 99,5 purity, from Sigma-Aldrich) were used as received without any treatment or further purification. All cell culture chemicals and supplies were acquired from Merck and Sigma Aldrich.

### 3.2 - Electrospinning

The polymer solution with a polymer concentration of 10 wt% was prepared by dissolving PLA and GE with different weight ratios: 3:0 1:3, 1:1, 3:1 of 0:3 (PLA:GE ratio) in HFIP. The solution was stirred for 12 h at room temperature and subsequently transferred to a glass syringe (10 mL) fitted with a steel needle with 0.41 mm inner diameter (gauge 22). Electrospinning was conducted at an applied electrical field of  $1.7 \text{ kV}\cdot\text{cm}^{-1}$  with a high voltage power supply from *Gamma High Voltage Research*. A syringe pump (KDS 100L Pump from *KDScientific*) was used to feed the polymer solutions into the needle tip at a rate of  $0.5 \text{ ml}\cdot\text{h}^{-1}$ . The electrospun fibres were collected on a grounded collecting plates (random fibres) placed at a distance of 15 cm from the needle.

The electrospun membranes were recorded in accordance with the name in the table 3.1. The letter "P" represents PLA and "G" represents gelatine, and the number represented the weight ratio of PLA and GE.

**Table 3.1** – Description of membranes developed according to the weight ratio of PLA and gelatine.

Sample Name	PLA amount (w/w)	GE amount (w/w)
PLA	100	0
PG31	75	25
PG11	50	50
PG13	25	75
GE	0	100

### 3.3 - Cross-linking

Electrospun fibres were placed 48 h in a vapour chamber containing 20 ml of GA. To convert unreacted aldehyde groups remaining in the GA to carboxylic acid, the membranes were immersed in 100 mmol glycine aqueous solution during 30 min at pH 7 and thoroughly washed with phosphate buffered saline (PBS) (pH= 7.4, at room temperature) to remove residual solvents. Then, the membranes were placed immediately in the freezer at -80°C. Finally, the membranes were freeze dried in a vacuum freeze-drying machine overnight [47].

### 3.4 - Materials Characterization

The characterization of the membranes was performed through several techniques including scanning electron microscopy (SEM), water angle contact (WCA) Fourier transform infrared (FT-IR) spectroscopy, differential scanning calorimetry (DSC), thermogravimetric analysis (TGA), water retention capacity and cross-linking degree through UV-Vis measurements.

#### 3.4.1 - Scanning electron microscopy (SEM)

Electrospun fibres were coated with a thin gold layer using a sputter coating and their morphology was analysed using a scanning electron microscopy (SEM) (model JSM-6000 NeoScope, JEOL) with an accelerating voltage of 10 kV.

#### 3.4.2 - Diameter measurements

Based on the SEM images, nanofiber average diameter and distribution were measured with 50 arbitrarily selected fibres using the image visualization software *ImageJ* (<http://imagej.nih.gov/ij/>) [60].

### 3.4.3 - Determination of the degree of cross-linking

The degree of cross-linking of fish gelatine electrospun fibres was determined through UV-Vis measurements using a protein quantification kit (Protein Quantification Kit-Rapid, Sigma-Aldrich) that is based on Coomassie Brilliant Blue G (CBB), which reacts with free amino groups (NH<sub>2</sub>) remaining in the membranes after cross-linking and stains blue under acidic conditions. At first, the samples were weighted to obtain 1 mg of gelatine in all samples. Then, 150 µL of CBB solution was added to all the samples and the absorbance of the solution was measured for the spectral range 400-620 nm at 1 nm resolution with an ELISA reader (Synergy HT, Biotek). The optical absorbance of the gelatine powder was also measured. The amount of free amino groups in the sample test is proportional to the absorbance of the solution and was determined by comparison to a standard curve of BSA vs absorbance.

The degree of cross-linking was then calculated (XCL) according to equation n° 3.1, where “free” is the mole fraction of free NH<sub>2</sub> in the non-crosslinked samples and “fixed” is the mole fraction of free NH<sub>2</sub> remaining in the cross-linked samples [61].

$$X_{CL} = \frac{NHN \text{ reactive amine}_{fixed}}{NHN \text{ reactive amine}_{free}} \quad (3.1)$$

### 3.4.4 - Contact angle measurements

Water contact angle measurements (WCA, sessile drop in dynamic mode) were performed at room temperature in a Data Physics OCA20 device using ultrapure water as test liquid. The contact angles were measured by depositing water drops (3 µL) on sample surfaces and analysed with SCA20 software. At least 5 measurements were performed in each sample and in different membrane locations and the average contact angle was taken as the result for each sample.

### 3.4.5 - Swelling and water retention capacity

The swelling ratio denotes the water absorption percentage of the nanofibrous membranes at equilibrium. The capacities of water absorption were tested by immersing the electrospun fibres in deionized water at room temperature. The samples were then removed and placed between two pieces of tissue paper to remove excess of water. Water retention capacity was determined with the increase in the weight of the fibres through the equation n° 3.2, where  $W$  is the weight of the sample after submersion for a certain period of time and  $W_d$  is the weight of the sample in its dry state before submersion [62].

$$Swelling \ degree \ (%) = \frac{W - W_d}{W_d} \times 100\% \quad (3.2)$$

### 3.4.6 - Thermogravimetric analysis

Thermal degradation kinetics of the samples was characterized by thermogravimetric analysis (TGA) in a Q500 apparatus from *TAINstruments* at heating rate of 20 °C.min<sup>-1</sup>. All measurements were performed under a nitrogen atmosphere. Differential thermal curves were obtained from TGA curves by plotting a graph between derivate weight % and temperature.

### 3.4.7 - Differential scanning calorimetry

The thermal behaviour of the electrospun fibre mats were analysed by differential scanning calorimetry measurements (DSC) with a Mettler-Toledo DSC 823e apparatus. The samples were cut into small pieces from the middle region of the electrospun membranes and placed into 30 µl aluminium pans and heated between 30 and 200 °C at a heating rate of 10 °C.min<sup>-1</sup>. All experiments were performed under a nitrogen purge. The glass transition temperature ( $T_g$ ), cold-crystallization temperature ( $T_{cc}$ ) and melting temperature ( $T_m$ ) of the electrospun mats samples were evaluated.

### 3.4.8 - Fourier transform infrared spectroscopy

Infrared measurements (FT-IR) were performed at room temperature in a Shimadzu IRAffinity-1S apparatus in ATR mode from 4000 to 600 cm<sup>-1</sup>. FT-IR spectra were collected after 32 scans with a resolution of 2 cm<sup>-1</sup>.

## 3.5 - Cell culture procedure

To evaluate cell behaviour in the presence of the scaffolds, human fibroblasts were used for this experiment. Fibroblast cells were cultured in alpha minimum essential medium ( $\alpha$ -MEM) supplemented with 10% (v/v) fetal bovine serum (FBS), 1% (v/v) fungizone and 1% (v/v) penicillin-streptomycin incubated at 37°C, in a humidified atmosphere of 95% air and 5% CO<sub>2</sub>. The medium was changed every 3-4 days and sub-cultured once they reached 70-80% confluence. Detachment of adherent cells was achieved by a 10 min incubation with trypsin 0.05% in 0.25% EDTA solution, at 37°C. For cell culture, circular membranes with 13 mm diameter were previously sterilized in both sides by UV radiation for 30 min.

## 3.6 - Cell viability and proliferation

To evaluate the cytotoxicity, membrane samples were held at the bottom of the 24-well culture plate with Teflon inserts. Then, fibroblasts (passage 8) were seeded on the membranes at a cell density of 2x10<sup>4</sup> cells/well. Wells containing cells seeded without materials (n=3) and wells containing only culture medium with material (n=1) were used as controls.

Cell viability and proliferation of fibroblast cells on the membranes was estimated by the Resazurin cell viability assay, at days 1, 3, 7 and 14. Briefly, the medium was removed from

the wells and replaced by a mixture of 500  $\mu\text{L}$  of culture medium and resazurin solution (10%), in the dark. The samples were incubated at 37 °C, in a humidified atmosphere of 95% air and 5%  $\text{CO}_2$ , for 3h. The redox activity within the cytosol of the viable cells was assessed through the reduction of the Resazurin, a blue compound, into resorufin, which is red in colour [63]. Following, 100  $\mu\text{L}$  of the solution was transferred to a 96-well plate to read the fluorescence on an ELISA reader (Synergy HT, Biotek) at 530 nm excitation wavelength and 590 nm emission wavelength. The experiment was performed in triplicate for each group.

### **3.7 - Statistical analysis**

All quantitative results were expressed as mean  $\pm$  standard deviation (SD) of at least three replicates. Statistical differences were determined by performing two-way ANOVA analysis followed by Dunnett's multiple comparisons test using GraphPad, Prism Software (V.7). Differences were taken to be statistically significant when compared to control for each day for P values < 0.05.



# Chapter 4

## Results and Discussion

One of the main concerns regarding the tissue engineering process consists on the choice of biomaterials with the desired features to be used as scaffolds [64]. Good biocompatibility and sufficient mechanical strength are basic requirements for membranes in nerve regeneration [65]. When a single polymer does not have the properties desired for tissue engineering, a blend of polymers may be employed to achieve the desired geometrical, mechanical and biodegradation properties [15]. The electrospinning technique allows the ability to produce nanofibers of a polymeric blend. Electrospun nanofibers have been proven to be a promising scaffold in the field of tissue engineering [61] due to their dimension which are able to mimic the natural extracellular matrix, which play an essential role in structural integrity and mechanical robustness of the tissue construct. The electrospun nanofibrous membranes of PLA/GE meet the requirements by taking advantages of both material properties. GE is a natural component of the extracellular matrix that can provide a suitable ground for cell adhesion, proliferation and differentiation [66], whereas PLA provides good mechanical properties because of its slow degradation rate [38].

The selection of an appropriate solvent is essential to determine the rheological properties and the morphology of nanofibers [67]. In this work, PLA, fish gelatine and PLA blended with fish gelatine were electrospun into nanofibers using hexafluoroisopropanol (HFIP) as the solvent. The characteristics of the solvent, such as volatility and polarity, have important effects on the diameter and morphology of the fibres. The low surface tension of the HFIP allows the production of fibres with a smaller average diameter [50], which is known to be more desirable to mimic the structure of the natural extracellular matrix [55]. In addition, the use of HFIP gives more uniform and bead-free fibres [68].

### 4.1 - Morphology of the electrospun membranes

The morphology and structure of the membranes were observed using SEM. SEM is a powerful tool for characterizing the size, shape and structure of materials due to its ability to resolve nanometre scale features [69]. This is an important technique to characterize biomaterials topography that are known to influence the cell response [58].

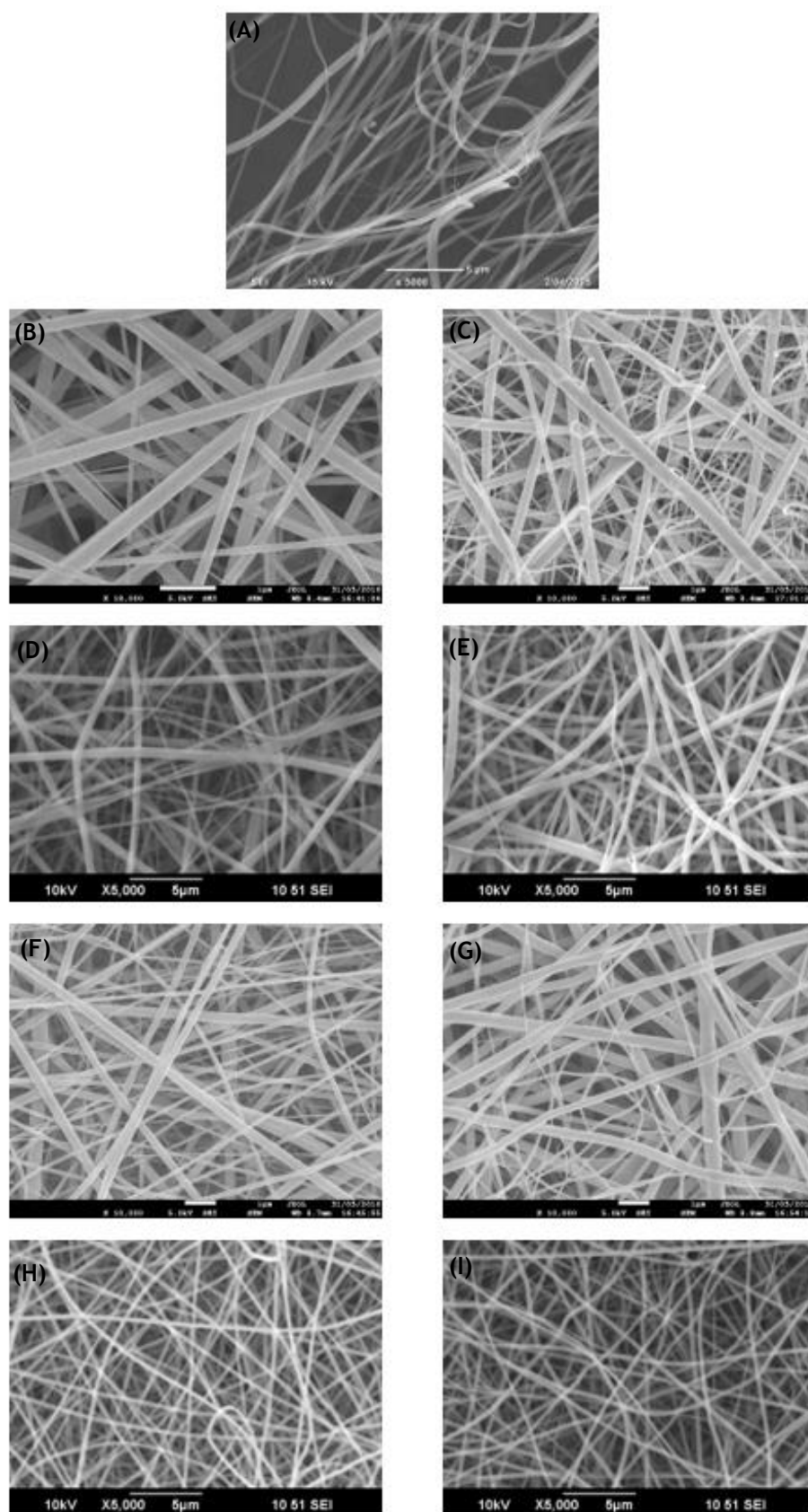


**Figure 4.1-** SEM morphologies of the electrospun polymeric nanofibers; (A) PLA, (B) PG31, (C) PG31 cross-linked, (D) PG11, (E) PG11 cross-linked, (F) PG13, (G) PG13 cross-linked, (H) GE and (I) GE cross-linked.

Figure 4.1 shows the representative SEM images of the electrospun nanofibers of PLA blended with GE at five different weight ratios. As it can be observed, the gelatine is uniformly distributed in the fibrous structure of the PLA and show to adhere strongly to the nanofibers of PLA. The electrospun fibres were generated into well-developed nonwoven nanofibers matrices. Beyond, nanofibers were bead-free strings with smooth surfaces.

As mentioned above, the obtained electrospun fibres are highly soluble in aqueous environments [61], which limits its applicability [70]. Therefore, to extend the application of gelatine fibres to procedures requiring contact with biological medium, gelatine fibres were exposed to a saturated atmosphere of GA in order to promote chemical cross-linking of the material. After cross-linking procedure, it was observed that the overall aspect of the cross-linked fibres (Figure 4.1-C, E, G, I) is maintained and no significant changes on fibre morphology were detected by SEM. Moreover, the electrospun membranes could sustain the cross-linking procedure and preserve their original morphologies. In addition, the membranes became visibly yellowish. The colour change is due to the establishment of aldimine linkages (CH=N) between the free amino groups of lysine or hydroxylysine amino acids residues of the protein and the aldehyde groups of glutaraldehyde [71].

In addition, based on the SEM images, the diameter of the nanofibers was measured using the ImageJ software. Fibre average diameter is an additional structural feature of electrospun scaffolds that can influence cellular interactions [58]. The evolution of average fibre diameter for untreated and cross-linked membranes is represented in figure 4.2.

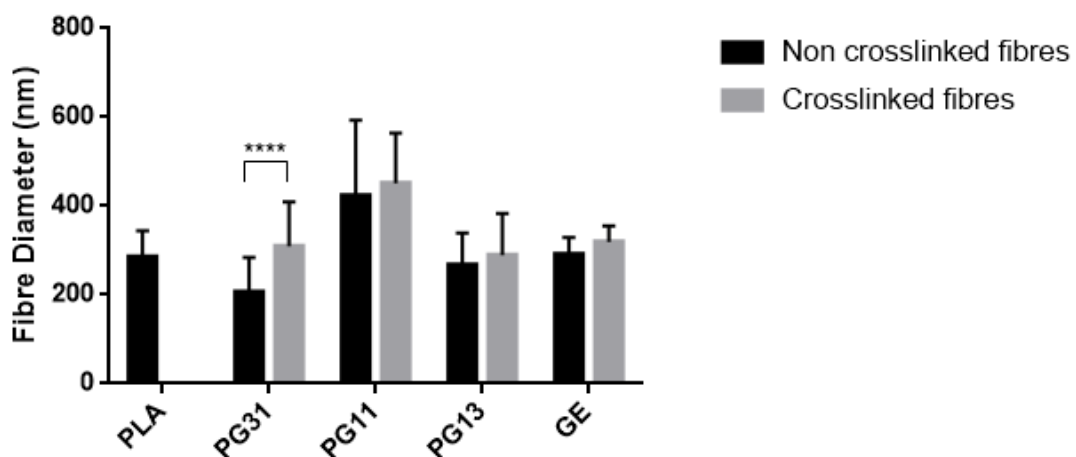


**Figure 4.2-** Evolution of fibre mean diameter for electrospun fibres samples before and after cross-linking; bars represent means  $\pm$  SD. Significant differences ( $p < 0.05$ ) between PG31 non-crosslinked and cross-linked membranes were found.

For the PLA, the fibre average diameter was  $285 \pm 59$  nm. Concerning the gelatine, the diameter increased slightly in relation to the PLA, obtaining an average diameter of  $292 \pm 37$  nm. It was observed that for the case of the PLA/GE electrospun polymer blend the average diameter varied from  $207 \pm 78$  to  $424 \pm 169$  nm depending on fibre compositions, and PG11 fibres had the highest diameter. The addition of gelatine in the PLA fibres caused the increase of the average fibre diameter, probably due to the deposition of the gelatine in the surface of the PLA fibres making a core-shell structure. The absence of a trend in fibre mean diameter

could indicate the occurrence of different interactions between the PLA and gelatine with the solvent.

Lastly, it was found that the cross-linking did not influence significantly the fibre diameter distribution, following the same trend as previously observed of the neat electrospun membranes. This effect was also observed by Padrão et al. for fish gelatine membranes [47].

## 4.2 - Degree of cross-linking

Glutaraldehyde was used in this study as a cross-linking reagent at the time of preparation of the electrospun membranes. GA is an organic compound widely used as cross-linker because its vapour phase is efficient and fast in stabilizing collagenous materials [46]. During the cross-linking, the reaction occurs between the free amine groups ( $-NH_2$ ) of lysine or hydroxylysine amino acid residues in the gelatine polypeptide chains and the aldehyde groups of GA [46] through a nucleophilic addition-type reaction, resulting in a more organized amorphous structure with more free space between the polymer network [49].

The objective was to make the as-electrospun gelatine nanofibers water insoluble through a GA cross-linking treatment so as to preserve their fibrous morphology and enhance their thermal and mechanical performance and to verify that GA was a favourable cross-linking reagent for gelatine electrospun membranes and can efficiently cross-link protein amino groups. The degree of cross-linking of the membranes was determined through UV-Vis measurements. The calibration curve of BSA protein was used to quantitatively determine the amount of free amino groups in the sample, thus calculating the degree of cross-linking of the membranes.

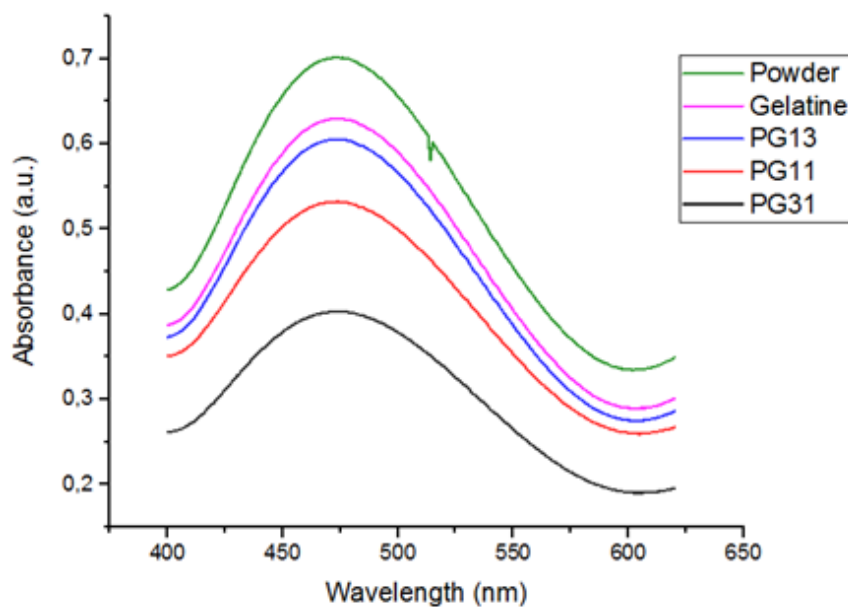


Figure 4.3 - Optical absorbance of the gelatine powder and the PLA/gelatine membranes.

In figure 4.3, it is represented the absorption spectrum of the gelatine powder (non-crosslinked raw material) and the cross-linked membranes. As it can be observed, the optical absorbance for the membranes is lower than the gelatine powder, which suggest that GA worked as a cross-linking agent.

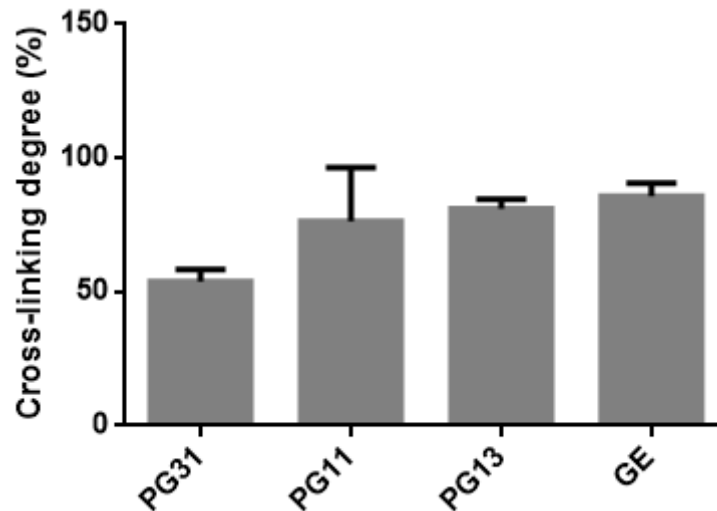


Figure 4.4 - Degree of cross-linking for gelatine and PLA/GE electrospun membranes.

The results showed a degree of cross-linking ranging from 54 to 86%. So, GA is a favourable cross-linking agent for gelatine electrospun membranes, as it can be efficiently cross-link protein amino groups.

### 4.3 - Contact angle measurements

Surface wettability is one of the most important parameters affecting the biological response, since wettability affects protein adsorption and cell adhesion [72]. The wettability of the membranes was evaluated by measuring the water contact angle (WCA).

Figure 4.5 shows that PLA membranes have a strong hydrophobic behaviour with WCA of  $136 \pm 1^\circ$ . Once gelatine is reported as superhydrophilic material [73], it was expected a lower contact angle for PLA/GE membranes compared to PLA membranes. In fact, a decrease of WCA was observed after the incorporation of GE. However, PL31 membranes shows a hydrophobic behaviour with WCA of  $134 \pm 1^\circ$ , despite the incorporation of GE. The fact that WCA of PG31 and PLA membranes was identical, indicate the embedment of GE component in the continuous PLA phase [17]. On the other hand, a significant difference between PG31 membranes and PG11 and PG13 membranes is observed. PG11, PG13 and GE membranes shows a hydrophilic behaviour with WCA of  $0^\circ$ . The PG13 membranes were suggested having a reverse microstructure to PG31 membranes that PLA component was separated and embedded in the continuous GE phase, for it containing more amount of GE component [17]. These results suggested that different structures had formed in fibres with different ratios of PLA and GE.

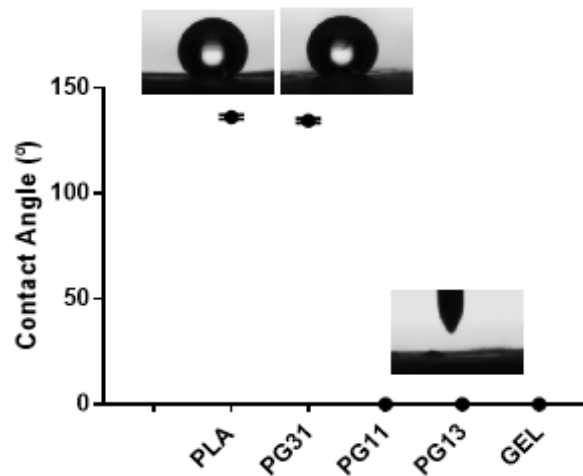


Figure 4.5 - Evolution of water contact angles for electrospun fibres membranes. Values are mean  $\pm$  SD.

In sum, the blending of PLA with gelatine clearly improved the hydrophilicity of the membranes. The hydrophilicity of membranes increased with the increase of GE amount. It is reported that biomaterial surfaces with moderate hydrophilicity show improved cell growth and higher biocompatibility [74].

#### 4.4 - Swelling Degree

The knowledge of the swelling degree is important for the predictions of stability and changes that may occur in biological environments [75]. The swelling ability of the membranes plays an important role during *in vitro* cultures. When the porous hydrogel is capable of swelling, it increases pore size thus facilitating the cell not only to attach but also to migrate inside the scaffold [76].

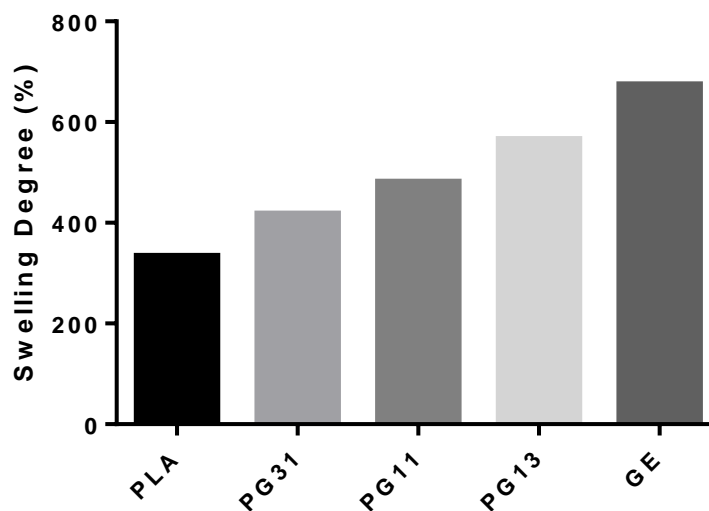


Figure 4.6 - Equilibrium swelling ratio of PLA/gelatine electrospun membranes with different blending compositions.

Figure 4.6 shows the swelling degree of the electrospun PLA, gelatine and the blends. As expected, gelatine exhibited the highest swelling degree and can absorb around 675% water after 1 minute immersed in deionized water, whereas the swelling degree of PLA was the lowest (335%). Since PLA is a hydrophobic polymer, the value of swelling degree obtained may be due to the water remained in its surface. Cross-linked gelatine is insoluble but swelling in aqueous environments. Gelatine easily absorbs water since it contains hydroxyl and amino groups, which affects their fibrous structure. In the case of the polymer blends, the swelling degree were found to be directly proportional to the concentration of gelatine in the membranes. It was observed that as the concentration of the gelatine increased, the degree of swelling also increased. In descending order, PG13 membranes showed a swelling degree of 566%. Then, PG11 membranes was the next one with a swelling degree of 482%. Finally, PG31 membranes showed a swelling degree of 418%.

Since PLA is a hydrophobic material (Figure 4.5), deionized water might not penetrate into the interior pores of the membranes and, consequently, the swelling degree is smaller. On the other hand, the hydrophilic gelatine (Figure 4.5) should accelerate the water absorption within the nanofiber network, increasing the swelling degree of the material.

The swelling degree of the PLA/gelatine blends could be attributed to the introduction of gelatine within PLA, since the degree increases when gelatine amounts also increase.

## 4.5 - Thermal behaviour

Thermogravimetric analysis (TGA) was used to characterize the thermal stability of the electrospun membranes. TGA is a technique in which the weight changes in a material are monitored as a function of temperature. The knowledge of the degradation mechanism is needed in order to optimize the processing conditions since TGA gives information about the highest processing temperature that can be employed and the study of kinetics of the decomposition process supports the identification of the decomposition mechanisms [77].

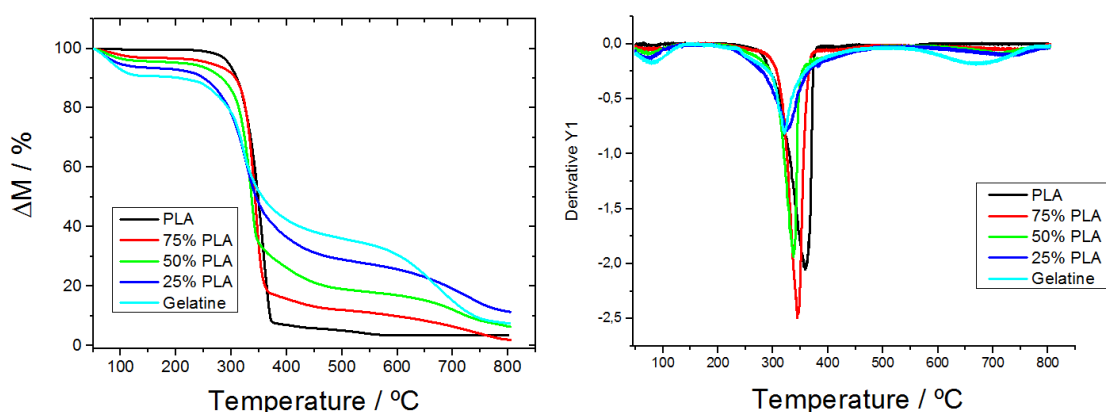


**Figure 4.7** - a) TGA data for pure PLA and GE samples, as well as for the PLA-GE and b) DTG curves for the obtained scaffolds.

Figure 4.7-a) shows the thermo-gravimetric analysis for PLLA, gelatine and blends. For the pure PLA, as expected, one single degradation process was observed which starts from around 260 °C and almost completed at 390 °C, which could be attributed to the chain scission of ester linkages [62].

Thermal degradation of gelatine occurs in three different stages. The first stage has been found at temperatures between 50 °C and 120 °C, which is related to the loss of absorbed and bound water due to the handling of the sample at room conditions without any special care. After its initial weight loss, gelatine was found to be quite stable until the temperature reached 230 °C. The second stage occurred between 230 °C and 450 °C and gelatine sample exhibited a large drop in weight due to the protein degradation and peptide bond rupture. Lastly, the third stage was found between 450 °C and 750 °C, which corresponds to the thermal decomposition of the gelatine networks [47,78].

Different from gelatine, the hydrophobic polymers did not undergo any degradation between 40 and 100 °C, indicating the absence of water molecules [61].

In the case of the polymer blends, it was observed in TGA curves of all blend polymers an initial decrease in weight due to moisture loss from the gelatine portion. Then, the blends showed a large decrease in weight at approximately the same temperature as that pure PLA. However, the blends degrade more slowly than PLA due to the presence of gelatine [69]. The blend samples had degradation temperatures between those of pure PLA and gelatine.

The derivative curves of weight loss for PLA, gelatine and PLA/gelatine blends are shown in figure 4.7- b). Each peak represents the  $T_{max}$  which corresponds to the maximum degradation rate at particular temperature [47]. In derivative thermogravimetric (DTG) analysis, gelatine and PG13 membranes both exhibit two peaks. Gelatine shows the maximum degradation rate at 83 °C and 321 °C, while PG13 membranes at 79 °C and 326 °C. PLA, PG13 and PG11 membranes show only one single peak of fast thermal degradation at 358 °C in PLA, 344 °C in PG31 membranes and 337 °C in PG11 membranes.

According to Lewandowska, when the measured lower  $T_{max}$  of one component shifts to the higher  $T_{max}$  of another component then it shows some interactions between polymer components in the blend [79] and, consequently, an improved thermal stability could be achieved for the component with a lower  $T_{max}$  [80]. In this work, in the blend polymers, lower  $T_{max}$  of gelatine has shifted to the higher  $T_{max}$  of PLA that indicates some interactions between PLA and gelatine in the blend polymers.

Differential scanning calorimetry (DSC) was used to measure the thermal properties of the electrospun membranes. Figure 4.8 shows DSC heating scans performed on electrospun PLA, gelatine as well as for the electrospun blends.

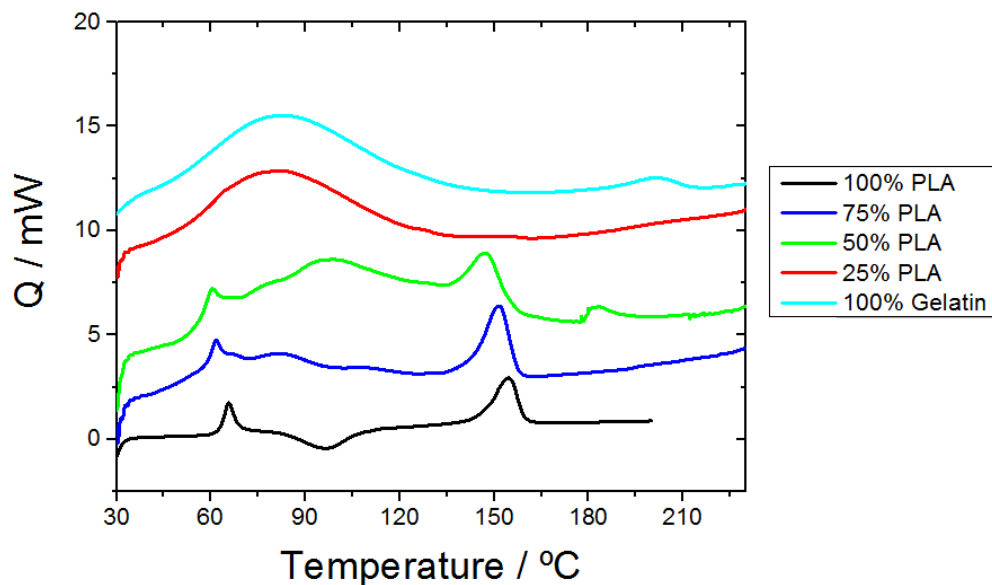


Figure 4.8 - DSC thermograms for electrospun fibres samples.

Since PLA is a slowly crystallizing polymer and with glass transition above room temperature which implies that the samples collected at room temperature maintain a stable crystalline fraction [81]. The DSC thermogram obtained for PLA samples shows that the polymer exhibits a large overshoot in the region of the glass transition ( $T_g$ ) around  $66^\circ\text{C}$ . This endothermic peak can be attributed to the recovering of enthalpy of sample stored at room temperature below  $T_g$  and, consequently, subjected to physical ageing [62]. Cold crystallization ( $T_{cc}$ ) starts immediately above glass transition and corresponds to the broad exothermic peak between  $80$ - $110^\circ\text{C}$ , with a minimum at  $96^\circ\text{C}$ . The temperature of cold crystallization immediately above the glass transition temperature indicate that numerous crystal nuclei were already present in the glass [17]. Melting ( $T_m$ ) starts in the region between  $140$ - $162^\circ\text{C}$ .

The DSC thermogram obtained for gelatine shows a broad endothermic peak in the range of  $30$ - $160^\circ\text{C}$ , with a maximum at  $85^\circ\text{C}$ , which have often been termed as denaturation temperature ( $T_D$ ) [71]. This peak is associated with the evaporation of bound water that was previously absorbed by the polymer when in contact with air [47]. In addition, an endothermic shoulder was observed at  $200^\circ\text{C}$ , associated to the amorphous structure of random coil conformations and lower contents of helical conformations [82]. The gelatine was amorphous since no gelatine melting peak appeared in DSC scans [69]. A previous study [13] on electrospun fibres revealed that the PLA are nearly amorphous.

Miscibility of the pure polymers in the blend can be determined by the measurement of the variation of  $T_g$  with the change of the weight fraction of the blend. A single glass transition temperature for a polymer blend, located between the glass transition temperature of the polymer components is an indication of polymer miscibility [81,83]. In this study, the electrospun PG31 and PG11 samples exhibited the thermal properties of the pristine polymers

and,  $T_g$  and  $T_m$  of the PG31 and PG11 appearing in the same positions as the PLA and gelatine, which shows that the blending of the materials is difficult to detect.

Regarding to PG13 samples, the DSC thermogram obtained a broad endothermic peak in the range of 30-130°C, with a maximum at 82°C. These results indicated that the polymer blends samples exhibited a similar structure of pure components of the blends in proportion to the ratio between both components. In addition, it was found an occurrence of a single broad peak in the cases of PG13 membranes. The occurrence of a single broad peak in a blended system indicated the limited interaction between the two constituent polymers.

## 4.6 - Infrared spectra

FT-IR spectrometer was used to characterize chemical structure and conformation of the electrospun membranes [69]. The infrared spectrum is formed by absorption of electromagnetic radiation at frequencies that correspond with specific groups of chemical bonds of a molecule. Each spectral band is characterized by its frequency and amplitude [36,84]. The FT-IR technique was used to evaluate if the introduction of the gelatine in the PLA solution lead to some chemical modification and, also, the compatibility between the polymers.

Figure 4.9 shows the FT-IR spectrum of electrospun nanofibers. For PLA fibres, the characteristic absorption bands are clearly observed at 1752  $\text{cm}^{-1}$  which represents C=O stretching band [16, 42, 50, 68, 85-87], and the C-O from carboxyl groups and C-O=C stretching vibration characteristic of ester bonds at 1182 and 1083  $\text{cm}^{-1}$  [16,50,85]. The spectrum also contained moderate intensity peaks from the methyl group, including C-H asymmetric deformation vibration at 1456  $\text{cm}^{-1}$  [16, 50, 69] and C-H symmetric deformation vibration at 1382  $\text{cm}^{-1}$  [16, 69, 84].

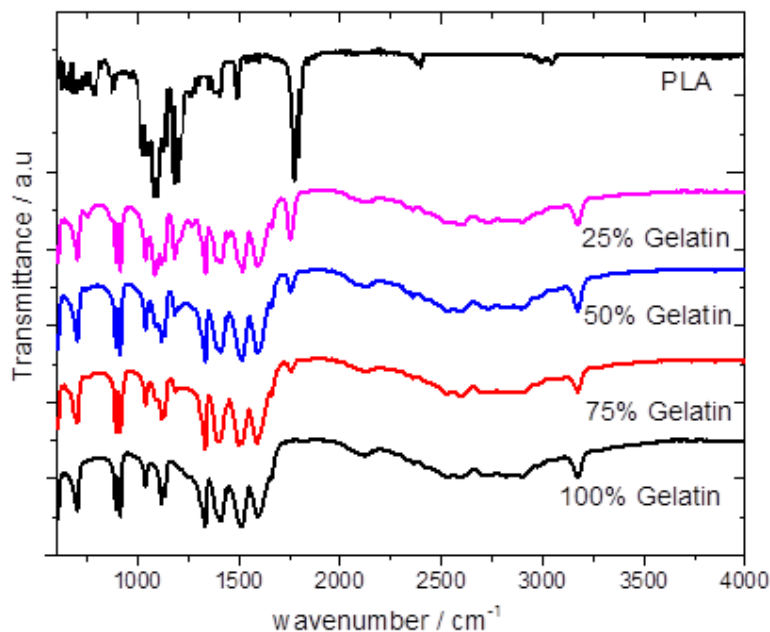


Figure 4.9 - FT-IR spectra for the pure PLA, pure gelatine and the PLA/GE blend membranes.

The gelatine spectrum contained the two main functional groups, the amide I peak at 1591  $\text{cm}^{-1}$ , which derived from C=O stretching vibrations, and the amide II peak at 1515  $\text{cm}^{-1}$ , which derived from a combination of N-H deformation and C-N stretching vibrations [16, 50, 51, 61, 69, 80, 88-90]. Another broad peak with moderate intensity at 3173  $\text{cm}^{-1}$  was attributed to the contributions of amide A related to N-H and OH-H stretching vibrations and intermolecular hydrogen bonding [16, 50, 61, 80, 87-89]. Additionally, the band at 1333  $\text{cm}^{-1}$  is attributed predominantly to the wagging vibration of proline side chains [87].

For PLA/gelatine blends fibres, in addition to the PLA characteristic peaks, the two amide peaks are also visible. However, the spectra of the blends exhibited the characteristic absorption bands of pure components of the blends in proportion to the ratio between both components and there were no shifts in these peaks position, which would indicate that the molecular interactions between gelatine and PLA were weak. The weak bonds are due to PLA does not have enough -OH groups to form hydrogen bonds with -OH and -NH<sub>2</sub> groups in gelatine [92].

These results indicated that gelatine had been incorporated into PLA electrospun membranes and the blend fibres were mixed physically. Beyond, infrared measurements do not reveal any new vibrational modes in the polymeric blends, what supports the phase separation of the two polymers in the blend.

Furthermore, the evolution of the infrared spectra can be used to control the development of crystallinity in the polymer. Although some vibration frequencies have fixed frequencies, others frequencies shift between the amorphous and crystalline  $\alpha$  and  $\alpha'$  forms [17]. The frequencies obtained to PLA in the infrared spectrum corresponds to that of amorphous PLA, in good agreement with DSC results (Figure 4.8).

FT-IR results are supported by TGA and DTG results (Figure 4.7).

**Table 4.1** - Infrared bands associated with different phases of PLA (Adapted from [13]).

IR frequency ( $\text{cm}^{-1}$ )	Phase form	Band assignment	Reference No.
1082	$\alpha'$ and $\alpha$	$\nu_s(C - O - C)$	[13,16,19,50,84]
1182	Amorphous $\alpha'$ and $\alpha$	$\nu_{as}(C - O - C) + r_{as}(CH_3)$	[13,16,50,63,87]
1387	Amorphous	$\delta_s(CH_3)$	[13,16,69,85]
1454	Amorphous	$\delta_{as}(CH_3)$	[13,16,50,69]
1752	$\alpha$	$\nu(C = O)$	[13,16,42,50,63,69,85-87]

**Table 4.2** - FT-IR spectra characteristics of fish gelatine.

IR frequency ( $\text{cm}^{-1}$ )	Region	Band assignment	Reference No.
3173	Amide A	$\nu_{NH}, \nu_{OH}$	[16,50,61,80,87,90-91]
1591	Amide I	$\nu_{C=O}, \nu_{NH}$	[16,51,61,69,80, 88-91]
1515	Amide II	$\delta_{NH}, \nu_{C-N}, \nu_{C-C}$	[16,51,60,69,80,88-90]

## 4.7 - Cell viability and proliferation

The cytocompatibility of PLA, gelatine and blend membranes was characterized through *in vitro* studies. Cytocompatibility is necessary in cell-scaffold interaction, since cell adhesion, proliferation and spreading on scaffold contribute crucially tissue regeneration [50]. Sample morphology play an important role in regulating cellular behaviour and cell attachment. A series of biological reactions, such as nutrient supply, initial protein binding and cell adhesion should be favorably affected by the nanofibrous structure [16]. Furthermore, to achieve this goals we used PLA blended with gelatine to improve the hydrophilicity of the membranes.

To asses the behaviour of cells seeded over the electrospun membranes, we analysed adhesion and proliferation of fibroblasts cells that were cultured for 14 days over the developed membranes. Fibroblast are intrinsic constituents of all three major compartments, such as epineurium, perineurium and endoneurium [93]. After a peripheral nerve injury, Schwann cells initiate proliferation and migration and participate actively with accumulated fibroblasts at the injury site establishing a guidance channel, called Bands of Bungner, crucial for peripheral nerve regeneration [94].

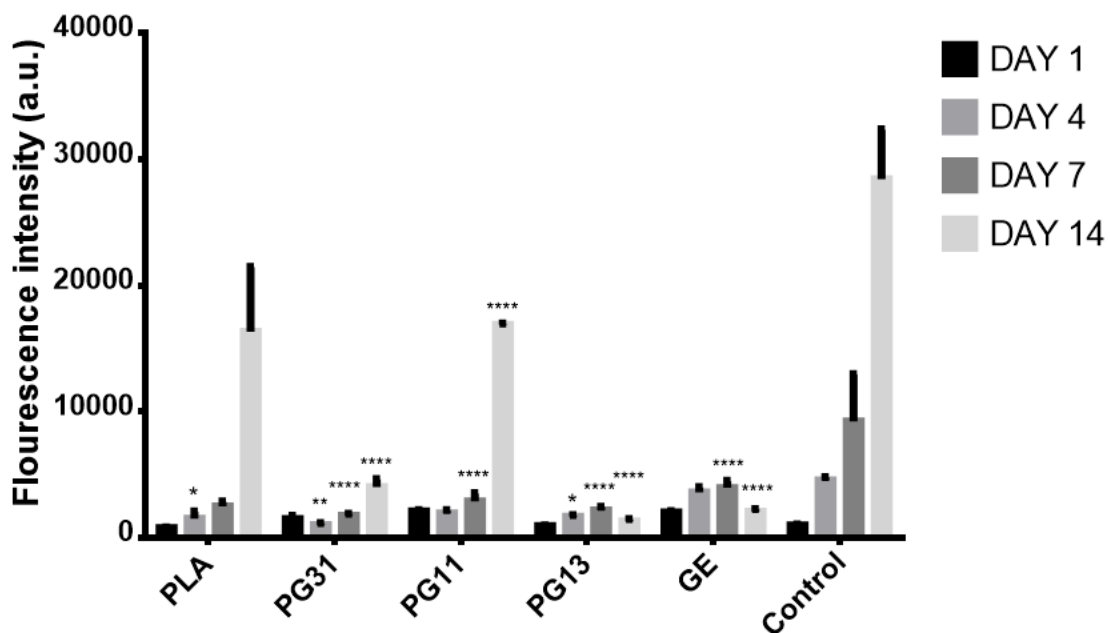


**Figure 4.10** - Resazurin viability of fibroblast cells after 1, 4, 7 and 14 days of being seeded. “PLA” cells seeded in PLA membranes; “PG31” cells seeded in PG31 membranes; “PG11” cells seeded in PG11 membranes; “PG13” cells seeded in PG13 membranes; “GE” cells seeded in gelatine membranes. Each result is presented as the mean  $\pm$  SD of four replicates. Statistical analysis was performed using two-way ANOVA with Dunnet’s post hoc test being the significant differences when compares to control for each day (\*  $p < 0.05$ ).

Although the hydrophobic interaction between PLA and GE could prevent the complete dissolution of GE from the composite, cross-linking treatment was still necessary before the PLA/GE electrospun membrane were used for cell culture. In this study, cell culture experiments were carried out on electrospun membranes cross-linked with GA. However, although the cross-linking treatment improved the water-resistant ability and thermal-mechanical properties of electrospun gelatine membranes, an adverse effect is that such treatment could be cytotoxic to cellular growth during *in vitro* and *in vivo* experiments [95]. Thus, it is necessary a treatment with an efficient removal of unreacted GA left in the material after the cross-linking treatment. After the glycine treatment, it was found that fibre morphology of gelatine membranes could not be preserved. The membrane loses their fibrous structure and became a polymeric film.

The redox activity of viable cells after 1, 4, 7 and 14 days in culture is shown in figure 4.10 by the resazurin cell viability assay. In this study, it was verified that cell adhesion and proliferation of fibroblasts cells is different in the membranes with different weight ratios of PLA and gelatine.

In the first 24 hours, cell adhesion and proliferation was noticed in wells where cell were in contact with materials and in the control. The metabolic activity of fibroblast cells culture in the electrospun membranes is similar when compared to the control. After 4 days of culture is observed a slight inhibition in metabolic activity of cells cultured in the PG13 and PG11 membranes when compared to the day 1. Cells continued to proliferate in wells in contact with PLA, PG31 and gelatine membranes. After 7 days of cell culture, it is observed an increase on cell proliferation in all membranes compared to the day 4. At this time point, cell metabolic activity is similar for all the membranes, however lower than that obtained in control. After 14 days, cells seeded in the presence of PG13 and gelatine membranes showed that in both cases cell viability decreased and cells in wells containing PG31 membranes presented the lowest proliferation. As previously mentioned, gelatine membrane loses their fibrous structure and became a polymeric film. The cellular responses to the substrate with nanolevel morphology are understood to be very different. The differences obtained between electrospun membranes and polymeric films were due to the higher porosity of the electrospun membranes [48]. Since gelatine films had lower porosity and the porous structure provide a large surface area that will allow cell ingrowth, the lower cell viability may be related to porosity.

Additionally, there is a remarkable increase in cell proliferation on the PG11 membranes after 14 days of culture when compared to the other membranes and probably this behaviour is related to the fibre diameter. S.J. Eichhorn et al. [96] determined that an increase in fibre diameter resulted in an increase in mean pore radius. Larger pores may be required for ingrowth of the cells into the nanofibrous network. In this study, PG11 electrospun membranes had the highest diameter (Figure 4.2), which should facilitate better penetration of cells into the membrane, leading to the difference of cell viability compared with other blended membranes (PG13 and PG31 membranes).

The PG11 electrospun membranes was proven to be a good substrate for cell culture compared to pure PLA and GE, since their morphology was improved. In fact, the PLA modification with gelatine could improve the viability and attachment of fibroblasts. This finding suggest that the PLA/GE blend should have better potential for use in the tissue regeneration.



# Chapter 5

## Conclusions and Future Work

### 5.1 - Conclusions

Peripheral nerve repair is one of the most difficult problems in the field of neuroscience. Currently, the gold standard for peripheral nerve injury repair is surgical implantation of autologous nerve grafts. However, there are several disadvantages associated with this technique. These problems drive the search of different solution to substitute autologous nerve grafts [97]. The use of NGC is a promising alternative to traditional techniques [98]. Nerve regeneration can be improved by increasing the surface area for cell growth into the nerve conduit. This can be achieved using electrospun nanofibers that provide a large surface area and a number of pores similar to a natural ECM, which is favourable to cell adhesion and proliferation [99].

In this context, this dissertation thesis describes a method using biomaterials to enhance peripheral nerve regeneration. To accomplish this, the development of electrospun membranes as well as their characterization were achieved. Due to the hydrophobic properties of the PLA, the blending of these with natural polymers, such fish gelatine, which possess better biological properties was tried. PLA/GE blends with different weight ratios were successfully electrospun from the solution of polymers in a common solvent (HFIP). The gelatine has been incorporated into PLA membranes and the blend fibres were mixed physically. In order to improve stability in aqueous environments, chemical cross-linking with GA was performed for 48h, and it was found that the cross-linking treatment does not influence the fibre morphology. In addition, it was found that the nanofibrous membranes were properly cross-linked. The average fibre diameter obtained were in the range of 207-452 nm, found to be more desirable to mimic the natural extracellular matrix (50-500 nm) [100]. The introduction of gelatine within PLA significantly improved the hydrophilic property of the nanofibers. In fact, the blending process leads to a decrease on polymer wettability and creates superhydrophilic membranes when higher gelatine amounts are added to the solution. In the electrospun membranes a swelling phase was observed, which can be important for cell survival.

After the development and characterization of PLA/GE was achieved, the biological response was addressed. Appropriate cytocompatibility is the foremost concern when a biomaterial is used for tissue regeneration purpose. From the evaluation of the *in vitro* results,

it appears that PG11 membranes offer the best conditions for fibroblast cell adhesion and proliferation. PG11 membranes could support fibroblast growth and proliferation, which suggested that the membranes had good cytocompatibility, whereas cells cultures on the PG31 and PG13 membranes had low viability.

These results suggest that the blend polymers PG13 and PG31 do not possess the ideal properties for a good cellular adhesion and proliferation, thus being their use impractical in the tissue regeneration field. On the other hand, from the structural and biological analysis, the PG11 membranes seem to be suitable and in some way ideal to promote the nerve regeneration, since their properties were considerably improved after modification. In this experimental work was developed a simple but efficient modification enhancing the potential application of electrospun membranes in the field of peripheral nerve regeneration.

## 5.2 - Future Work

These tests indicate that the incorporation of gelatine in PLA membranes has the potential to enhance cell adhesion and proliferation but further research is necessary to better characterize the membranes and its biological functions. Optimization of the glycine treatment of the membranes should be performed to maintain the membrane morphology. Furthermore, a future work will be important to evaluate mechanical properties of the membranes.

The other issue to improve material cellular behaviour is to cross-link the gelatine with more biocompatible crosslinking agents such EDC/NHS or genipin.

While fibroblasts cells represent a suitable model to evaluate the cytotoxicity of the membranes, these cells do not represent the behaviour of Schwann cells. Since the proliferation of these cells is crucial for successful peripheral nerve regeneration, further viability tests should be performed using Schwann cells for comparison.

Finally, each developed biomaterial should be evaluated *in vivo* through the use of animal models. The rat model provides a realistic and useful model of damage for the study of peripheral nerve regeneration. Nerve guidance conduits should be constructed and implanted to evaluate its potential in peripheral nerve regeneration. Essential parameters such as inflammation, cellular proliferation and differentiation, functional testing must be investigated.

## References

- [1] P. A. S. Armada-da-Silva, C. Pereira, S. Amado, A. Luís and A.C. Maurício, “Activity-Based Strategies in the Rehabilitation of Peripheral Nerve Injuries”, *Intech*, pp. 52-66, 2014.
- [2] D. Grinsell and C.P. Keating, “Peripheral Nerve Reconstruction after Injury: A Review of Clinical and Experimental Therapies”, *Hindawi*, pp. 1-13, 2014.
- [3] A. Faroni, S. A. Mobasser, P. J. Kingham and A. J. Reid, “Peripheral Nerve Regeneration: Experimental Strategies and Future Perspectives”, *Advanced Drug Delivery Reviews*, pp. 160-167, 2014.
- [4] X. Gu, F. Ding and D. F. Williams, “Neural tissue engineering options for peripheral nerve regeneration”, *Biomaterials*, pp. 6143-6156, 2014.
- [5] V. Carriel, M. Alaminos, I. Garzón, A. Campos and M. Cornelissen, “Tissue engineering of the peripheral nervous system”, *Expert Review Neurother*, pp.301-318, 2014.
- [6] A. Atala, R. Lanza, J. A. Thomson and R. M. Nerem, “Foundations of Regenerative Medicine”, *Academic Press*, 1<sup>st</sup> edition, pp. 672-683, 2010.
- [7] X. Gu, F. Ding, Y. Yang and J. Liu, “Construction of tissue engineered nerve grafts and their application in peripheral nerve regeneration”, *Progress in Neurobiology*, pp. 204-230, 2011.
- [8] W. W. Campbell, “Evaluation of peripheral nerve injury”, *European Journal of Pain Supplements*, pp. 37-40, 2009.
- [9] Y. Shirotsaki, S. Hayakawa, A. Osaka, M. A. Lopes, J. D. Santos, S. Geuna and A. C. Mauricio, “Challenges for Nerve Repair using Chitosan-Siloxane Hybrid Porous Scaffolds”, *Hindawi*, pp. 1-7, 2014.
- [10] C.W. Patrick, A. G. Mikos and L. V. McIntire, “Frontiers in Tissue Engineering”, *Pergamon*, 1<sup>st</sup> edition, pp. 514-535, 1998.
- [11] D. Shi, “Biomaterials and Tissue Engineering”, *Springer*, 1<sup>st</sup> edition, pp. 195-234, 2004;
- [12] Y. Shirotsaki, K. Tsuru, S. Hayakawa, A. Osaka, M. A. Lopes, J. D. Santos and M. H. Fernandes, “In vitro cytocompatibility of MG63 cells on chitosan-organosiloxane hybrid membranes”, *Biomaterials*, pp. 485-493, 2005.
- [13] C. Ribeiro, V. Sencadas, C. M Costa, J. L. G. Ribelles and S. Lanceros-Méndez, “Tailoring the morphology and crystallinity of poly(L-lactide acid) electrospun membranes”, *Science and Technology of Advanced Materials*, pp. 1-9, 2011.
- [14] B. Dhandayuthapani, Y. Yoshida, T. Maekawa and D. S. Kumar, “Polymeric Scaffolds in Tissue Engineering Applications: A Review”, *Hindawi*, pp. 1-19, 2011.
- [15] C. P. Barnes, S. A. Sell, E. D. Boland, D. G. Simpson and G. L. Bowlin, “Nanofiber technology: Designing the next generation of tissue engineering scaffolds”, *Advanced Drug Delivery Reviews*, pp. 1413-1433, 2007.

- [16] HW. Kim, HS. Yu and HH Lee, "Nanofibrous matrices of poly(lactic acid) and gelatin polymeric blends for the improvement of cellular responses", *Wiley Periodicals*, pp. 25-32, 2007.
- [17] X. Yang, Q Xu, N. Yan, G. Sui, Q. Cai and X. Deng, "Structure and wettability relationship of coelectrospun poly(L-lactic acid)/gelatin composite fibrous mats", *Polymers Advanced Technologies*, pp. 2222-2230, 2011.
- [18] "Seeley's Anatomy and Physiology", 10<sup>th</sup> edition.
- [19] J. Ryu, C. F. Beimesch, T. J. Lalli, "Peripheral Nerve Repair", *Orthopedics and trauma*, pp. 174-180, 2011.
- [20] M. Richner, M. Ulrichsen, S. L. Elmegaard, R. Dieu, L. T. Pallesen and C. B. Vaegter, "Peripheral Nerve Injury Modulates Neurotrophin Signaling in the Peripheral and Central Nervous System", *Mol Neurobiol*, pp. 945-970, 2014.
- [21] C. A. Health and Gregory E. Rutkowski, "The development of bioartificial nerve grafts for peripheral-nerve regeneration", *Tibitech*, pp. 163-168, 1998.
- [22] H. J. Seddon, "A classification of nerve injuries", *British Medical Journal*, pp. 237-239, 1942.
- [23] Y. Kaya and L. Sarikeioghu, "Sir Herbert Seddon (1903-1977) and his classification scheme for peripheral nerve injury", *Childs Nervous System*, pp. 177-180, 2015.
- [24] A. Chhabra, S. Ahalawat and G. Andreseik, "Peripheral nerve injury grading simplified on MR neurography: As referenced to Seddon and Sunderland classifications", *The Indian Journal of Radiology and Imaging*, pp. 217-224, 2014.
- [25] A. Osbourne, "Peripheral Nerve Injury and Repair", *Reviews: Surgery*, pp. 29-35, 2007.
- [26] R. Deumens, A. Bozkurt, M. F. Meek, M. A. E. Marcus, E. A.J. Joosten, J. Weis and G. A. Brook, "Repairing injured peripheral nerves: Bridging the gap", *Progress in Neurobiology*, pp. 245-276, 2010.
- [27] C. V. Blitterswijk, "Tissue Engineering", *Academic Press*, 1<sup>st</sup> Edition, pp., 2008.
- [28] K. S. Straley, C. W. P. Foo and C. Heilshorn, "Biomaterial Design Strategies for the Treatment of Spinal Cord Injuries", *Journal of Neurotrauma*, pp. 1-19, 2010.
- [29] G. R.D. Evans, "Peripheral Nerve Injury: A Review and Approach to Tissue Engineered Constructs", *The Anatomical Record*, pp. 396-404, 2001.
- [30] F. J. O'Brien, "Biomaterials and Scaffolds for Tissue Engineering", *MaterialsToday*, pp. 88-95, 2011.
- [31] S. Kehoe, X.F. Zhang and D. Boyd, "FDA approved guidance conduits and wraps for peripheral nerve injury: A review of materials and efficacy", *Injury*, pp. 553-572, 2012.
- [32] G.C.W. Ruiter, M.J.A. Melessy, M. J. Yaszemski, A.J. Windebank and R. J. Spinner, "Designing ideal conduits for peripheral nerve repair", *Neurosurgical focus*, pp. 1-50, 2009.
- [33] S. Ichihara, Y. Inada, T. Nakamura, "Artificial nerve tubes and their application for repair of peripheral nerve injury: an update of current concepts", *Injury*, pp. 29-39, 2008.
- [34] X. Jiang, S. H. Lim, HQ. Mao, S. Y. Chew, "Current applications and future perspectives of artificial nerve conduits", *Experimental Neurology*, pp. 86-101, 2010.
- [35] L. Xiao, B. Wang, G. Yang and M. Gauthier, "Poly(Lactic Acid)-Based Biomaterials: Synthesis, Modification and Applications", *Intechop*, pp. 247- 282, 2012.
- [36] S. Ramakrishna, K. Fujihara, WE. Teo, TC. Lim and Z. Ma, "An Introduction to Electrospinning and Nanofibers", *World Scientific*, 2005.
- [37] D. Arslantunali, T. Dursun and V. Hasirci, "Peripheral nerve conduits: technology update", *Medical Devices*, pp. 405-424, 2014.

- [38] R. M. Rasal, A. V. Janorkar and D. E. Hirt, "Poly(lactic Acid) modifications", *Progress in Polymer Science*, pp. 338-356, 2010.
- [39] A.J.R. Lasprilla, G.A.R. Martinez, B.H. Lunelli, A.L. Jardini and R.M. Filho, "Poly-lactic acid synthesis for application in biomedical devices- A review", pp.321-328, 2012.
- [40] V. Sencadas, C. Ribeiro, A. Heredia, I.K. Bdikin, A.L. Kholkin, S. Lanceros-Mendez, "Local piezoelectric activity of single poly(L-lactic acid) (PLLA) microfibers", *Applied Physics A*, pp. 51-55, 2012.
- [41] B. Gupta, N. Revagade, J. Hilbron, "Poly(lactic acid) fiber: An overview", *Progress in Polymer Science*, pp. 455-482, 2007.
- [42] G.S. Nyanhongo, R.D. Rodríguez, E.N. Prasetyo, C. Caparrós, C. Ribeiro, V. Sencadas and S. Lanceros-Mendez, E.H. Acero, and G.M. Guebitz, "Bioactive albumin functionalized polylactic acid membranes for improved biocompatibility", *Reactive and Functional Polymers*, pp. 1399-1404, 2013.
- [43] C. Ribeiro, V. Sencadas, D.M. Correia and S. Lanceros-Mendez, "Piezoelectric polymers as biomaterials for tissue engineering applications", *Colloids and Surfaces B: Biointerfaces*, pp. 46-55, 2015.
- [44] L.M. Marquardt and S.E. Sakiyama-Elbert, "Engineering peripheral nerve repair", *Current opinion in Biotechnology*, pp. 887-892, 2013.
- [45] A.H. Rajabi, M. Jaffe and T.L. Arinze, "Piezoelectric materials for tissue regeneration: A review", *Acta Biomaterialia*, pp. 12-33, 2015.
- [46] S.R. Gomes, G. Rodrigues, G.G. Martins, C.M.R. Henriques and J.C. Silva, "In vitro evaluation of crosslinked electrospun fish gelatin scaffolds", *Materials Science and Engineering C*, pp. 1219-1227, 2013.
- [47] D.M. Correia, J. Padrão, L.R. Rodrigues, F. Dourado, S. Lanceros-Mendez and V. Sencadas, "Thermal and hydrolytic degradation of electrospun fish gelatin membranes", *Polymer Testing*, pp. 995-1000, 2013.
- [48] A. Kejing, L. Haiying, G. Shidong, D.N.T. Kumar and W. Qingqing, "Preparation of fish gelatin and fish gelatin/poly(L-Lactide) nanofibers by electrospinning", *International Journal of Biological Macromolecules*, pp. 380-388, 2010.
- [49] J. Padrão, J.P. Silva, L. R. Rodrigues, F. Dourado, S. Lanceros-Méndez and V. Sencadas, "Modifying Fish Gelatin Electrospun Membranes for Biomedical Applications: Cross-Linking and Swelling Behavior", *Soft Materials*, pp. 247-252, 2014.
- [50] E. Hoveizi, M. Nabiuni, K. Parivar, S. Rajabi-Zeleti and S. Tavakol, "Functionalisation and surface modification of electrospun polylactic acid for tissue engineering", *Cell Biology International*, pp. 41-49, 2014.
- [51] A. Etxabide, M. Urdanpilleta, P. Guerreiro and K. Caba, "Effects of cross-linking in nanostructure and physicochemical properties of fish gelatins for bio-applications", *Reactive and Functional Polymers*, pp. 55-62, 2015.
- [52] S. Panzavolta, M. Gioffre, M.L. Focarete, C. Gualandi, L. Foroni and A. Bigi, "Electrospun gelatin nanofibers: Optimization of genipin cross-linking to preserve fiber morphology after exposure to water", *Acta Biomaterialia*, pp. 1702-1709, 2011.
- [53] J. Ratanavaraporn, R. Rangkupan, H. Jeeratawatchai, S. Kanokpanont and S. Damrongsakkul, "Influences of physical and chemical crosslinking techniques on electrospun type A and B gelatin fiber mats", *International Journal of Biological Macromolecules*, pp. 431-438, 2010.

- [54] V. Beachley, X. Wen, "Polymer nanofibrous structures: Fabrication, biofunctionalization and cell interactions", *Progress in polymer science*, pp. 868-892, 2010.
- [55] S. Agarwal, J.H Wendorff and A. Greiner, "Use of electrospinning technique for biomedical applications", *Polymer*, pp. 5603-5621, 2008.
- [56] D. Kai, S.S. Liow, X.J. Loh, "Biodegradable polymers for electrospinning: Towards biomedical applications", *Materials Science and Engineering C*, pp. 659-670, 2014.
- [57] A. Baji, YW. Mai, SC. Wong, M. Abtahi and P. Chen, "Electrospinning of polymer nanofibers: Effects on oriented morphology, structures and tensile properties", *Composites Science and Technology*, pp. 703-718, 2010.
- [58] R.J. Wade and J.A. Burdick, "Advances in nanofibrous scaffolds for biomedical applications: From electrospinning to self-assembly", *NanoToday*, pp. 722-742, 2014.
- [59] M. Ziabari, V. Mottaghitab and A.K. Haghi, "Application of direct tracking method for measuring electrospun nanofiber diameter", *Brazilian Journal of Chemical Engineering*, pp. 53-62, 2009.
- [60] C. A. Schneider, W. S. Rasband and K. W. Eliceiri, "NIH Image to ImageJ: 25 years of image analysis", *Nature Methods*, pp. 671-675, 2012.
- [61] J. Padrão, R. Machado, M. Casal, S. Lanceros-Méndez, L.R. Rodrigues, F. Dourado and V. Sencadas, "Antibacterial performance of bovine lactoferrin-fish gelatine electrospun membranes", *International Journal of Biological Macromolecules*, pp. 608-614, 2015.
- [62] N. Nagiah, R. Johnson, R. Anderson, W. Elliott and W. Tan, "Highly compliant vascular grafts with gelatin-sheathed coaxially structured nanofibers", *Langmuir*, pp. 1-10, 2015.
- [63] T. A. M. Valente, D. M. Silva, P. S. Gomes, M. H. Fernandes, J. D. Santos and V. Sencadas, "Effect of sterilization methods on electrospun poly(lactic acid) (PLA) fibre alignment for biomedical applications", *ACS Applied Materials and Interfaces*, pp. 1-26, 2016.
- [64] T. Nie, L. Xue, M. Ge, H. Ma and J. Zhang, "Fabrication of poly(L-lactic acid) tissue engineering scaffolds with precisely controlled gradient structure", *Materials Letters*, pp. 25-28, 2016.
- [65] A. Subramanian, U. M. Krishnan and S. Sethuraman, "Development of biomaterial scaffold for nerve tissue engineering: Biomaterial mediated neural regeneration", *Journal of Biomedical Science*, pp. 1-11, 2009.
- [66] H. Duan, B. Feng, X. Guo, J. Wang, L. Zhao, G. Zhou, W. Liu, Y. Cao and W. J. Zhang, "Engineering of epidermis skin grafts using electrospun nanofibrous gelatin/polycaprolactone membranes", *International Journal of nanomedicine*, pp. 2077-2084, 2013.
- [67] R. Casasola, N.L. Thomas, A. Trybana and S. Georgiadou, "Electrospun poly lactic acid (PLA) fibres: Effect of different solvent system on fibre morphology and diameter", *Polymer*, pp. 4728-4737, 2014.
- [68] J. Kucinska-Lipka, I. Gubanska, H. Janik and M. Sienkiewicz, "Fabrication of polyurethane and polyurethane based composite fibres by the electrospinning technique for soft tissue engineering of cardiovascular system", *Materials Science and Engineering C*, pp. 166-176, 2015.
- [69] BS. Chiou, H. Jafri, R. Avena-Bustillos, K.S. Gregorski, P.J. Bechtel, S.H. Imam, G.M. Glenn and W.J. Orts, "Properties of electrospun Pollock gelatin/poly(vinyl alcohol) and Pollock gelatin/poly(lactic acid) fibers", *International Journal of Biological Macromolecules*, pp. 214-220, 2013.

- [70] A. Laha, S. Yadav, S. Majumdar and C. S. Sharma, “In-vitro release study of hydrophobic drug using electrospun cross-linked gelatin nanofibers”, *Biochemical Engineering Journal*, pp. 481-488, 2016.
- [71] Y. Z. Zhang, J. Venugopal, Z. M. Huang, C. T. Lim and S. Ramakrishna, “Crosslinking of the electrospun gelatin nanofibers”, *Polymer*, pp. 2911-2917, 2006.
- [72] C. Ribeiro, J.A. Panadero, V. Sencadas, S. Lancers-Méndez, M.N. Tamanõ, D. Moratal, M. Salmerón-Sánchez and J.L.G. Ribelles, “Fibronectin absorption and cell response on electroactive poly(vinylidene fluoride) films”, *Biomed. Mater.*, pp. 1-10, 2012.
- [73] J. Zhu, F. Yang, F. He, X. Tian, S. Tang and X. Chen, “A tubular gelatin scaffold capable of the time-dependent controlled release of epidermal growth factor and motimycin C”, *Colloids and Surfaces B: Biointerfaces*, pp. 416-424, 2015.
- [74] C. Ribeiro, S. Moreira, V. Correia, V. Sencadas, J. G. Rocha, F. M. Gama, J. L. Gómez Ribelles and S. Lancers-Mendez, “Enhanced proliferation of pre-osteoblastic cells by dynamic piezoelectric stimulation”, *RSC Advances*, pp. 11504-11509, 2012.
- [75] S. F. Hosseini, Z. Javidi and M. Rezaei, “Efficient barrier properties of multi-layer films based on poly(lactic acid) and fish gelatine”, *International Journal of Biological Macromolecules*, pp. 1205-1214, 2016.
- [76] J. Araujo, J. Padrão, J. P. Silva, F. Dourado, D. M. Correia, G. Botelho, J. L. Gomez Ribelles, S. Lancers-Méndez and V. Sencadas, “Processing and characterization of  $\alpha$ -elastin electrospun membranes”, *Applied Physics A: Materials Science and Processing*, pp. 1291-1298, 2014.
- [77] V. Sencadas, C. M. Costa, G. Botelho, C. Caparrós, C. Ribeiro, J. L. Gómez-Ribelles and S. Lancers-Mendez, “Thermal properties of electrospun poly(lactic acid) membranes”, *Journal of Macromolecular Science, Part B: Physics*, pp. 411-424, 2012.
- [78] S. Gautam, C. Chou, A. K. Dinda, P. D. Potdar and N. C. Mishra, “Surface modification of nanofibrous polycaprolactone/gelatin composite scaffold by collagen type I grafting for skin tissue engineering”, *Materials Science and Engineering C*, pp. 402-409, 2014.
- [79] K. Lewandowska, “Miscibility and thermal stability of poly(vinyl alcohol)/chitosan mixtures”, *Thermochimica Acta*, pp. 42-48, 2009.
- [80] S. Gautam, A. K. Dinda and N. C. Mishra, “Fabrication and characterization of PCL/gelatin composite nanofibrous scaffold for tissue engineering applications by electrospinning method”, *Materials Science and Engineering C*, pp. 1228-1235, 2013.
- [81] C. Ribeiro, V. Sencadas, C. Caparros, J. L. Gómez Ribelles and S. Lancers-Méndez, “Fabrication of Poly(lactic acid)-Poly(ethylene oxide) electrospun membranes with controlled micro to nanofiber sizes”, *Journal of Nanoscience and Nanotechnology*, pp. 6746-6753, 2012.
- [82] C. S. Ki, D. H. Baek, K. D. Gang, K. H. Lee, I. C. Um and Y. H. Park, “Characterization of gelatin nanofiber prepared from gelatin-formic acid solution”, *Polymer*, pp. 5094-5102, 2005.
- [83] A. Wagner, V. Poursorkhabi, A. K. Mohanty and M. Misra, “Analysis of porous electrospun fibers from Poly(L-lactic acid)/Poly(3-hydroxybutyrate-co-3-hydroxyvalerate) blends”, *ACS Sustainable Chemistry and Engineering*, pp. 1976-1982, 2014.
- [84] D. Duydu, T. Baykal, I. Açikgoz and K. Yildiz, “Fourier transform infrared (FT-IR) spectroscopy for biological studies”, *G.U. Journal of Science*, pp. 117-121, 2009.

- [85] R. Al-Itry, K. Lamnawar and A. Maazouz, "Improvement of thermal stability, rheological and mechanical properties of PLA, PBAT and their blends by reactive extrusion with functionalized epoxy", *Polymer Degradation and Stability*, pp. 1898-1914, 2012.
- [86] CS. Wu and HT. Liao, "A new biodegradable blends prepared from polylactide and hyaluronic acid", *Polymer*, pp. 1017-10026, 2005.
- [87] W. H. Hoidy, M. B. Ahmad, E. A. J. Al-Mulla and N. A. B. Ibrahim, "Preparation and Characterization of Polylactic Acid/Polycaprolactone Clay Nanocomposites", *Journal of Applied Sciences*, pp. 97-106, 2010.
- [88] M. J. Hossan, M. A. Gafur, M. R. Kadir and M. M. Karim, "Preparation and characterization of gelatin-hydroxyapatite composite for bone tissue engineering", *International Journal of Engineering and Technology*, pp. 1-9, 2014.
- [89] C. S. Ki, D. H. Baek, K. D. Gang, K. H. Lee, I. C. Um and Y. H. Park, "Characterization of gelatin nanofiber prepared from gelatin-formic acid solution", *Polymer*, pp- 5094-5102, 2005.
- [90] H. Staroszczyk, K. sztuka, J. Wolska, A. Wojtasz-Pajak and I. Kolodziejska, "Interactions of fish gelatin and chitosan in uncrosslinked and crosslinked with EDC films: FT-IR study", *Spectrochimica Acta Part A: Molecular and Biomolecular Spectroscopy*, pp. 707-712, 2014.
- [91] S. F. Hosseini, M. Rezaei, M. Zandi and F. F. Ghavi, "Preparation and functional properties of fish gelatin-chitosan blend edible films", *Food Chemistry*, pp. 1490-1495, 2013.
- [92] A. Kejing, L. Haiying, G. Shidong, D.N.T. Kumar and W. Qingqing, "Preparation of fish gelatin and fish gelatin/poly(L-lactide) nanofibers by electrospinning", *International Journal of Biological Macromolecules*, pp. 380-388, 2010.
- [93] L. Dreesmann, R. Mittnacht, M. Lietz and B. Schlosshauer, "Nerve fibroblasts impact on Schwann cell behavior", *European Journal of Cell Biology*, pp. 285-300, 2009.
- [94] N. Niapour, A. Niapour, H.S. Milan, M. Amani, H. Salehi, N. Najafzadeh and M.R. Gholami, "All trans retinoic acid modulates peripheral nerve fibroblasts viability and apoptosis", *Tissue and Cell*, pp. 61-65, 2015.
- [95] Q. Li, X. Wang, X. Lou, H. Yuan, H. Tu and B. Li, "Genipin-crosslinked electrospun chitosan nanofibers: Determination of crosslinking conditions and evaluation of cytocompatibility", *Carbohydrate Polymers*, pp. 166-174, 2015.
- [96] S.J. Eichhorn and W. Sampson, "Statistical geometry of pores and statistics of porous nanofibrous assemblies", *Journal of the Royal Society Interface*, pp. 309-318, 2005.
- [97] P.M. Jenkins, M.R. Laughter, D.J. Lee, Y.M. Lee, C.R. Freed and D. Park, "A nerve guidance conduit with topographic and biochemical cues: potential application using human neural stem cells", *NanoScale Research Letters*, pp. 10:264, 2015.
- [98] YL. Wang, XM. Gu and YM. Yang, "Electrospun and woven silk fibroin/poly(lactic-coglycolic acid) nerve guidance conduits for repairing peripheral nerve injury", *Neural Regeneration Research*, pp. 1635-1642, 2015.
- [99] S.Y. Park, C.S. Ki, Y.H. Park, K.G. Lee, S.W. Kang, H.Y. Kweon and H.J. Kim, "Functional recovery guided by an electrospun silk fibroin conduit after sciatic nerve injury in rats", *Journal of Tissue Engineering and Regenerative Medicine*, pp. 66-76, 2015.
- [100] I. O. Smith, X. H. Liu, L. A. Smith and P.X. Ma, "Nanostructured polymer scaffolds for tissue engineering and regenerative medicine", *WIREs Nanomedicine and Nanobiotechnology*, pp. 226-236, 2009.

## Appendix A

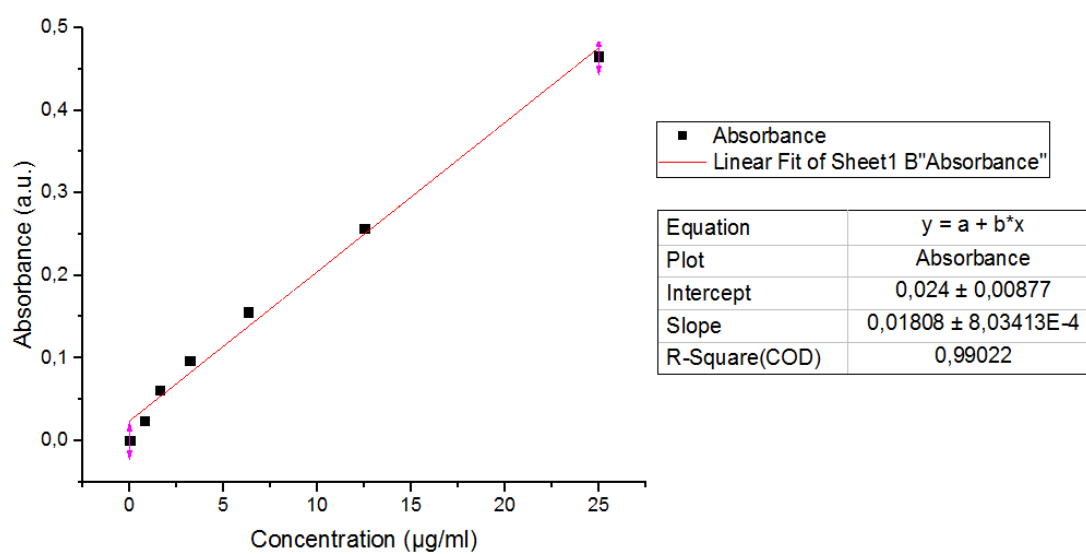


**Figure A.1** - Calibration curve of BSA protein used to determine the amount of free amino groups in the sample to calculate the degree of cross-linking.